

IMPROVING WORKABILITY OF IN-SITU ALUMINIUM COMPOSITES

A DISSERTATION

*Submitted in partial fulfillment of the
requirements for the award of the degree*

of

MASTER OF TECHNOLOGY

In

METALLURGICAL AND MATERIALS ENGINEERING

(With Specialization in Physical Metallurgy)

By

AMANDEEP SINGH DHIMAN



DEPARTMENT OF METALLURGICAL AND MATERIALS ENGINEERING

INDIAN INSTITUTE OF TECHNOLOGY ROORKEE

ROORKEE – 247667 (INDIA)

MAY, 2016

CANDIDATE'S DECLARATION

I hereby declare that the work presented in this dissertation entitled “**Improving Workability of Insitu Aluminium Composites**” in partial fulfillment of the requirement for the award of the degree of **Masters of Technology in Metallurgical and Materials Engineering** with specialization in **Physical Metallurgy**, submitted in the **Department of Metallurgical and Materials Engineering, Indian Institute of Technology, Roorkee** is an authentic record of my own work carried out during the period from July 2015 to May 2016 under the supervision of **Dr. B.S.S. Daniel**, Professor, Department of Metallurgical and Materials Engineering, Indian Institute of Technology, Roorkee.

The matter presented in this dissertation has not been submitted by me for the award of any other degree.

Dated:

Place: Roorkee

(AMANDEEP SINGH DHIMAN)

CERTIFICATE

This is to certify that above statement made by the candidate is correct to the best of my knowledge and belief.

Dr. B.S.S. Daniel

Professor

MMED, IIT Roorkee

Roorkee-247667 (INDIA)

ACKNOWLEDGEMENT

I would like to thank the almighty God for giving me strength to accomplish my work with honor. I am highly indebted to **Dr. B.S.S. Daniel**, Professor, Metallurgical and Materials Engineering, Indian Institute of Technology Roorkee, for encouraging me to undertake this dissertation as well as providing me all the necessary guidance and inspirational support throughout this dissertation work. He has displayed unique tolerance and understanding at every step of progress. It is my proud privilege to have carried out this dissertation work under his able guidance.

I wish to express my sincere thanks to **Dr. Anjan Sil**, Professor and Head of the Department, Metallurgical and Materials Engineering Department, Indian Institute of Technology Roorkee, for his help to carry out this dissertation.

I also like to express my gratitude to Mr. Rahul Gupta, Mr. Himanshu Kala Research Scholar for their innumerable discussion, his generosity and willingness to share his knowledge. I sincerely appreciate his valuable persistent encouragement in making this work.

I would like to acknowledge all my friends for their valuable information share, and developing love and confidence in me throughout the work. Last but not the least I would like to thanks my parents who have been a constant source of my inspiration to me.

AMANDEEP SINGH DHIMAN

ABSTRACT

In the past few decades, materials research has shifted from conventional materials to composite materials, adjusting to the global need for reduced weight, high quality, and high performance with low cost in structural materials. Metal matrix composites (MMCs) are emerging as an important class of materials for various applications in structural, automobile, aerospace and transportation industries. Aluminium metal matrix composites possess significantly improved properties like high specific strength, better specific modulus, damping capacity and good wear resistance compared to unreinforced alloys. In-situ aluminium based metal matrix composites are one of the most promising alternatives for eliminating the inherent defects or demerits associated with ex-situ reinforced composites.

The present work is an attempt to study the workability of in-situ Al6061/TiB₂ composite. Workability is the extent to which a material can be deformed without the formation of cracks. Products made by forming of aluminium MMCs (such as by forging, rolling, extrusion) find interesting industrial applications. The composite was manufactured through the in-situ process involving the salt-metal reaction between the titanium and boron salts (K₂TiF₆, KBF₄) and then casted into a permanent mould by ultrasonic assisted stir casting route. Hot-Compression tests of Al6061 - 5 wt. % TiB₂ with strain rate ranging from 0.001 s⁻¹ to 1 s⁻¹ and the deformation temperature ranging from 300 °C to 450 °C have been performed on Gleeble-3800 thermo mechanical simulator. Tensile and Hardness tests were also done on the samples prepared from the manufactured composites. The flow stress in hot deformation testing shows an increase in the stress with increase in strain rate and decrease in deformation temperature. Further, activation energy for the hot deformation is also found by the constitutive equation for the hot deformation which is 193.44 kJ/mol/K. Microstructural examination of composites before and after the hot-compression tests was done by XRD, SEM and EDX analysis.

CONTENTS

CHAPTER 1: INTRODUCTION	1
1.1 Why Composites?	1
1.2 Classification of Composites.....	1
1.3 Metal Matrix Composites (MMCs).....	2
1.4 Processing of Metal Matrix Composites	3
CHAPTER 2: LITERATURE SURVEY.....	5
2.1 Historical Background.....	5
2.2 Survey on Aluminium MMCs and Aluminium alloys	6
2.3 In-situ Composites and its properties	8
2.4 Processing of In-situ Aluminium MMCs	9
2.4.1 Ultrasonic Assisted Stir Casting technique	9
2.4.2 In situ Synthesis of reinforcement particles	12
2.5 Survey on Workability Studies of Aluminium MMCs	13
2.5.1 Workability and Processing Maps	13
2.5.2 Metallurgical factors effecting workability	15
2.5.3 Dynamic recovery and Dynamic recrystallization Phenomena.....	15
CHAPTER 3: PLAN OF WORK	17
CHAPTER 4: EXPERIMENTAL WORK	18
4.1 Material Selection	18
4.2 Fabrication of Al-TiB ₂ Composite	18
4.3 Tensile Test	21
4.4 Vickers Hardness Test.....	23
4.5 Scanning Electron Microscopy (SEM)	24
4.6 X-Ray Diffraction (XRD) Analysis	25

4.7 Hot Compression tests on TMS	26
CHAPTER 5: RESULTS AND DISCUSSION.....	28
5.1 Tensile Test Results	28
5.2 Hardness Measurement	29
5.3 X-Ray Diffraction Analysis (XRD)	30
5.4 SEM Images of the manufactured Al-TiB ₂ composite.....	32
5.5 Hot Compression Testing on TMS.....	34
5.5.1 True Stress-Strain Behavior.....	34
5.5.2 Constitutive Equation for the deformation of the composite	37
5.5.3 SEM Images of composite material after hot deformation tests	40
CHAPTER 6: CONCLUSION	49
CHAPTER 7: FUTURE SCOPE	50
REFERENCES	51

LIST OF FIGURES

Fig. 1 Classification of various types of composite materials [2].....	2
Fig. 2 Process of Stir Casting technique	11
Fig. 3 Ultrasonic Assisted Casting Process [6].....	11
Fig. 4 Process of In-Situ synthesis [6]	12
Fig. 5 Typical processing map. X-axis is temperature in degrees Celsius.	14
Fig. 6 Typical Plot of Dynamic recovery and recrystallization.	16
Fig. 7 Furnace used for the casting of in-situ Al composites.....	20
Fig. 8 Cast ingots of the composites manufactured in MMED department, IIT Roorkee	21
Fig. 9 Schematic diagram of a Tensile Sample.....	22
Fig. 10 Universal Testing Machine Model H-75 KS for tensile testing	22
Fig. 11 Computerized Vickers Hardness Tester in MMED, IIT Roorkee	23
Fig. 12 Scanning Electron Microscopy facility in MMED, IIT Roorkee	24
Fig. 13 Extraction process for XRD sample preparation.....	25
Fig. 14 Gleeble-3800 thermo mechanical-simulation facility in Materials and Metallurgy department, IIT Roorkee	27
Fig. 15 Stress-strain plots.....	28
Fig. 16 XRD patterns of in situ 9 wt. % Al-TiB ₂ composite	30
Fig. 17 XRD patterns of in-situ 3 wt. % Al-TiB ₂ composite fabricated by Ultrasonic assisted technique.....	31
Fig. 18 XRD patterns of in-situ 5 wt. % Al-TiB ₂ composite fabricated by Ultrasonic assisted technique.....	31
Fig. 19 SEM images and EDX analysis of produced Al6061/TiB ₂ composite (9 wt.%).	32
Fig. 20 SEM images and EDX analysis of Al6061/TiB ₂ composite formed by ultrasonic assisted technique (3wt.%)......	33
Fig. 21 True stress-true strain plots at strain rates (0.001 s ⁻¹ to 1 s ⁻¹): (a) 0.001 s ⁻¹ ; (b) 0.01 s ⁻¹ ; (c) 0.1 s ⁻¹ ; (d) 1 s ⁻¹ and at 300 °C, 350 °C, 400 °C, and 450 °C.	35
Fig. 22 True stress-true strain plots at constant temperatures (300 °C to 450 °C): (a) 300 °C; (b) 350 °C; (c) 400 °C; (d) 450 °C.	36

Fig. 23 Evaluating the value of (a) parameter n' by plotting $\ln \varepsilon$ versus $\ln \sigma$; (b) parameter by plotting $\ln \varepsilon$ versus σ ; (c) parameter n by plotting $\ln \varepsilon$ versus $\ln[\sinh(\alpha\sigma)]$; (d) the activation energy (Q) using the dependence of $\ln[\sinh(\alpha\sigma)]$ on $(1000/T)$	40
Fig. 24 SEM images of composite after hot deformation at 0.001 strain rate and different temperatures at 500X and 2000X magnification: (a) 350 °C; (b) 450 °C.	42
Fig. 25 SEM images of composite after hot deformation at 0.01 strain rate and different temperatures at 500X and 2000X magnification: (a) 300 °C; (b) 350 °C; (c) 400 °C; (d) 450 °C.	44
Fig. 26 SEM images of composite after hot deformation at 0.1 strain rate and different temperatures at 500X and 2000X magnification: (a) 300 °C; (b) 350 °C; (c) 400 °C; (d) 450 °C.	46
Fig. 27 SEM images of composite after hot deformation at 1 strain rate and different temperatures at 500X and 2000X magnification: (a) 300 °C; (b) 350 °C; (c) 400 °C; (d) 450 °C.	48

LIST OF TABLES

Table 1: Chemical composition of Al 6061[7]	7
Table 2: Standard Dimensions of Tensile Samples	21
Table 3: Stress-Strain Values	29
Table 4: Hardness values	29
Table 5: True Stress Values form the Stress Strain graphs at 0.4 true strain.....	38

The main purpose of manufacturing a composite material is to combine the properties of different materials in one material or, in other words, manufacturing one material which will have better properties than the original ones. Composite material is basically a material made up of two or more different materials, which will have a clear interface between the constituent materials [1]. Composite materials reveals a major portion of the properties in an excellent combination of properties for each of the constituent material present in that composite [2]. Composites shows vast applications in aerospace, and defense industries. This is because of their excellent properties like high specific strength and hardness, along with a good wear resistance property, and high strength-to-cost ratio, etc. Composite materials also have wide application in automotive industries [3, 4].

1.1 Why Composites?

The composites promises to supply huge business opportunities in comparison to region sector and this is due to its size in transportation industry. So, this has shifted the applications of composite materials from their normal uses to other sectors of business uses.

The reasons for using the composites are its excellent properties like increased stiffness, high strength and dimensional stability, high impact strength, increase in mechanical damping, scale back porosity, low cost, low thermal growth, better wear and corrosion resistance, light weight, good strength/stiffness at higher temperatures [4].

1.2 Classification of Composites

Classifications of the composites is done at two different levels. The first one or primary classification of composites is defined by the matrix constituent of the composite. These composite includes metal-matrix composites, ceramic-matrix and polymer-matrix composites [1].

Second level in classification of composites is based on the reinforcement type used in the composite: these include particle reinforced, fiber reinforced, and structural composites.

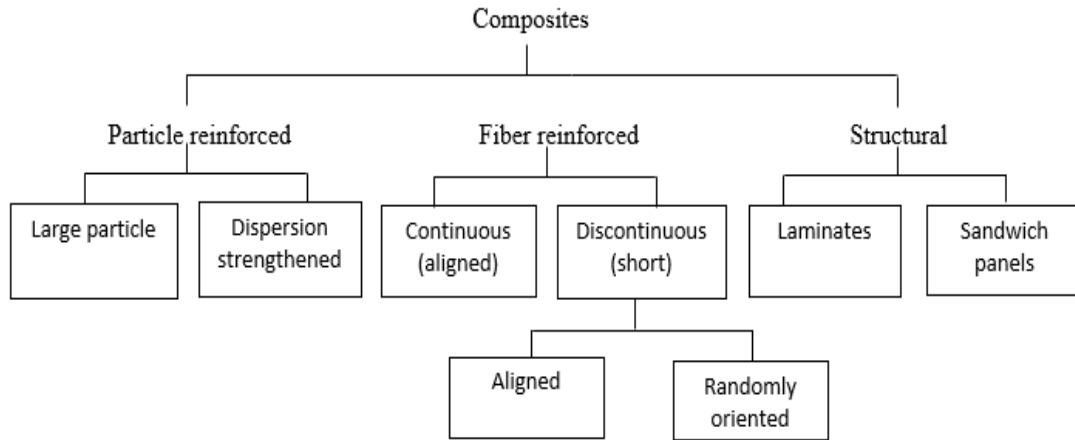


Fig. 1 Classification of various types of composite materials [2]

1.3 Metal Matrix Composites (MMCs)

MMCs emerged as an important class of structural materials for different applications like wear, and aerospace applications, and it is because of their great ability to have high strength to weight ratio along with the good strength to cost ratio [3]. The matrix constituent used in the MMC is generally a metallic alloy, and not the pure metal in most of the cases. There occurs three types of these composites, which include, dispersion-strengthened composites; matrix containing fine homogeneous particles with their diameters ranging from 10 to 100 nm, and particle-reinforced composites; in which the particle size is bigger than 1 μm , and fiber-reinforced; in which matrix contains the fibers that are continuous throughout the length of the matrix, or also it can be less than 1 μm long, and could be present in a wide range of volume fractions, 5 to 75% [3, 4].

In comparison to normal metals or metallic alloys, MMCs offers us far better properties like higher stiffness ratio, high wear resistance and corrosion resistance, also high temperature properties, low creep rate, high fatigue and lower coefficients of thermal growth with good strength to weight ratios [4, 5].

The advantages or merits of MMCs are as follows:

- Stabeness at high temperatures.
- Transversal strength and transversal stiffness is also high.
- Higher thermal conductivity and elctrical conductivity.

Some disadvantages or demerits of MMCs in comparison to the normal metals or alloys and other matrix composites are higher cost of some material systems, and a bit complex fabrication techniques for fiber-reinforced composite systems (except for casting methods).

1.4 Processing of Metal Matrix Composites

The temperature of the matrix constituent in the composite determines the fabrication process for most of the MMCs. These processes are thus classified in three categories that are:

- a) Liquid state processing,
- b) Solid-state processing, and
- c) Solid-liquid processing.

(A). Liquid state processes: These include squeeze castings, compo castings, stir castings, and ultrasonic assisted castings, in-situ (reaction) processing [6].

(B). Solid state processes: These include Powder metallurgy, high energy ball milling, friction Stir method, diffusion bonding and vapour deposition processing. The choice of the process route depends on the several factors as well as sort and level of reinforcement loading and therefore, the degree of microstructural integrity needed [6].

Stir Casting Process of MMCs

This method is liquid state processing technique used for the fabrication of composite materials, in which the reinforcement particles, or fibers are mixed into the molten metal or metallic alloy in the furnace with the help of mechanical stirrer. Standard casting methods are then used for the casting of the molten material present in the furnace and also it may be sometimes sent for post processing under standard metal forming techniques [4, 6].

Processing Variables and their effects

Rotation Speed:

The stirrer speed is very important for efficient production of composites by casting methods. Rotational speed affects the structure of final material formed, the common result by increasing the rotational speed being to push refinement and instability of the liquid alloy at terribly low speeds. Therefore, high speed should be used to reject the tearing problem if we see this logically.

Pouring Temperature:

Solidification process is greatly affected by the pouring temperature of the melt present in the furnace. Therefore, it should be carefully taken as it also depends on the structure of final product needed. If the temperature is kept low then it will give equiaxed structures and will also have max grain refinement whereas on the other hand when the temperature is high, it will lead to columnar growth in the cast products for some alloy systems. But if we see practically, we are restricted to some limits for keeping the temperature. So, the pouring temp in the furnace should be kept that much high which can avoid the formation of coarse structures and also be able for satisfactory flow of melt.

Metal dies are preferred over the other moulds for the casting. Required structure is not affected by the mould temperature. The only importance lies in the degree of growth in the die along with the pre-heating process. Any chance of tearing to occur in casting is diminished by the enlargement. Minimum 25 mm thickness should be kept for the mould.

Mould Coating:

Many kinds of coating materials can be used depending on the casting to be done. The internal surfaces of the metal mold are coated with the coating materials. Its main aim is to stop the heat transfer to the metallic mold. Shrinkage defects or cracks occurring in the molds are eliminated with the help of coating materials, therefore die life is also increased. Thickness of coating layer is changed to get the optimum value for all the different alloy melts. For aluminum alloys, most widely used coating is mixture of silicate and C in water.

2.1 Historical Background

In past years, there has been a new development on the composite materials. Area of structural design which needs higher strength with lower weight has tremendously increased the demand for better materials in comparison to the normal used materials [5]. Higher structural performance of any material can only increase the structural design efficiency. Aerospace accessories, and power instrumentation accessories etc. comes under the structural design applications. The key characteristic which is needed for the structural design applications is stiffness of any material. The other important characteristic of any structural material is their specific modulus, defined as ratio of elastic modulus to the density of material. Aluminum, titanium and steel are some very important structural engineering materials that have high specific modulus. Designers should always choose the low density structural materials for structural applications so as to increase the section size to get good bending stiffness with less weight. Considering all these issues, MMC shows promising category of structural materials form all the other different materials. MMCs are formed from at least two constituents or components which are metallic matrix (mostly alloys) and the hard reinforcements to increase the properties. The matrix is indicated as metal in the name MMC, but generally an alloy is used as a matrix instead of a pure metal matrix. Fabrication process of any composite includes the mixing of reinforcement material in the matrix material. MMCs have the ability to resist highly compressive stresses as it can transfer the load and distribute in the reinforcement particles or fibers that are reinforced in the matrix material. But, compositions and comparative amounts of matrix material and reinforcement material does not have very wide ranges and confined to a point which will be controlled by equilibrium conditions. MMCs can be fabricated by many different techniques like liquid metallurgy, compo casting, stir casting, etc. by intermixing the reinforcement material and matrix material [4, 5]. The reinforcements used are usually one of these following: continuous fibres of B or C and particulates like Al_2O_3 , SiC and TiB_2 which are discontinuous particles. The optimum

range for adding the reinforcement particles in the matrix is 10-30% volume fractions [5, 7].

2.2 Survey on Aluminium MMCs and Aluminium alloys

Need for better structural materials shifted the stress to investigate new light-weight materials with low cost and high performance along with high quality and which should also be eco-friendly. Considering all these points, MMCs are coming as an attracting materials [4, 5]. MMCs incorporate changes in the mechanical behavior i.e., increased tensile strength, high compressive strength, improved wear resistance and creep. It also changes the physical properties of the materials like density and thermal expansion. The development of MMCs has increased rapidly because of the need for advanced structural and engineering materials in different areas of automotive industries and also in the aerospace industries [5, 6]. Cost of the materials is also a crucial issue in the areas of transportation, and applications in automotive and aerospace industries.

Researchers are now more interested in particulate reinforced MMCs because of their isotropic properties and they are also cheaper [6]. These are also very useful in the applications where there is not much loading and no extreme thermal conditions are required. The industrial and processing issues concerned with continuous reinforcement composites are also contributing to the interest of researchers in the particulate reinforced MMCs. Because of the benefits of Al alloy like easier to handle and its low cost, these alloys are also very much preferred [7].

The ability of improving and governing the performance parameters that are related to the industrial processes makes MMC the most widely used class of structural composite materials. These are used as potential materials for numerous applications in automobile, transportation, avionics, and aerospace industries just because of their excellent mechanical properties and low thermal expansion co-efficient [5].

Al6061 alloy is the most widely used 6xxx series aluminium alloy which provides us a number of excellent mechanical properties, good surface finish, high workability, and higher wear resistance and excellent corrosion resistance [6]. A typical chemical composition of Al 6061 is given in Table 1 below. In recent, past researchers have used

wide selection of ceramic dispersoids like SiC [5, 7], B₄C, Si₃N₄ [6], Al₂O₃ [5] and TiO₂ as reinforcement materials in Al6061 based MMCs. However, in comparison to these dispersoids TiB₂ stands out as an excellent reinforcement, due to the fact that it possesses high hardness, high strength to density ratio and its resistive nature to avoid formation of interfacial reaction products with aluminium. Moreover, in comparison to most ceramics, TiB₂ reinforcements have higher electrical conductivity and also high thermal conductivity [7, 8].

Table 1 Chemical composition of Al 6061[7]

Element	Mg	Si	Fe	Cu	V	Mn	Ti	Al
Weight %	1.08	0.63	0.17	0.32	0.01	0.52	0.02	Remainder

When the melt containing the alloy matrix mixed with homogeneous distribution of reinforcement particles in the furnace solidifies then some interactions tends to occur between the particles and solidification front. These interactions effects the particle solidification and also the front morphology. The solidification front pushes the reinforcement particles and the particles are found at the grain boundaries, or in the interdendritic regions, or in the grains themselves. This phenomenon found in several solidification processes was ascertained by others also [9, 10]. The effect of particulate SiC reinforcement on the mechanical behavior of Al 6061 MMC has been previously studied by Srivatsan et. al. [10]. TiB₂ reinforcement particles synthesized by the in-situ salt metal reaction method are sometimes found to agglomerate and thus forming clusters. Feng and Froyen also reported the same finding in fabricating the aluminium composites with commercial pure Al as the matrix [11]. The in-situ based fabrication of the MMC under study was extensively reported within the literature [10-14]. However, production of the composite with Al 6061 as the matrix alloy containing TiB₂ as reinforcement is not widely reported.

But few works were carried out to introduce TiB_2 which is an excellent reinforcement among all the other reinforcements with aluminium metal matrix. This is often due to the very fact that TiB_2 reveals outstanding features like high melting point ($2790\text{ }^\circ\text{C}$), high hardness (86 HRA), high elastic modulus ($530 \times 10^3\text{ GPa}$) and excellent thermal stability. TiB_2 ceramic particles do not react with liquid aluminium, thereby avoiding formation of brittle reaction products at the reinforcements-matrix interfaces. Additionally, aluminium reinforced with TiB_2 is known for its good wear resistance property [7]. Christy [9] reported in his paper, "A Comparative study on microstructure, and mechanical properties of Al 6061 Alloy and the MMC Al 6061- TiB_2 /12% composite Al6061- TiB_2 /12% was successfully manufactured by the in-situ reaction procedure.

2.3 In-situ Composites and its properties

The composite materials in which the reinforcement is synthesized inside the matrix material while fabricating the composite is known as in-situ composite. Whereas in ex-situ composite materials, the reinforcements are produced separately and then incorporated in the matrix material using secondary processes like infiltration or powder processing. But the disadvantage of the ex-situ composite materials is the thermodynamical non-stability of reinforced material in the matrix material [6, 8]. In-situ composite processing methods therefore solve the problem we face with the ex-situ composite. Number of reinforcement morphologies can be produced from in-situ processes ranging from continuous to discontinuous. Reinforcement's used can be either of ceramic or ductile phases [8].

The advantages of in-situ composite materials in comparison to other ex-situ composites are:

- Particle size is small offering higher strength, improved fatigue resistance and creep.
- Single crystal reinforcements.
- Clear particle-matrix interfaces with high interfacial strength and improved wettability.
- Homogeneous distribution of reinforcement particles offering better mechanical and microstructural properties [9, 12].

In conclusion, the objectives to develop the in-situ particulate composites may be summarized as follows:

- The interfaces of the particle matrix are cleaner, because the particles separate out of the matrix. It will result in better interfacial bonding.
- Very fine particles might form within the matrix to produce dispersion hardened particle composites.
- The disadvantage of non-wettability of particles and interface degradation by chemical reaction, as discovered in synthetic composites can be ruled out.

The coherency of the in-situ formed reinforced particles with the matrix also helps in improving mechanical properties of in-situ composites. TiB_2 particles synthesized in the metallic matrix using in-situ technique offers very special advantages like clear matrix-particle interface leading to effective load transfer and minimizing the wear rates [7].

2.4 Processing of In-situ Aluminium MMCs

The most important thing in the fabrication of composite material is the homogeneous and uniform distribution of the synthesized reinforced particles so we can get defect free microstructures [8]. Size and shape of the reinforcement particles determines the nature of particles i.e., whether the reinforcements are particles or fibres. The low material cost and suitability for fast processing has made the particulate-reinforced composites more preferable as compared to the fiber-reinforced composites for automotive applications [9].

2.4.1 Ultrasonic Assisted Stir Casting technique

Stir casting method involves the mechanical stirring which is used for the homogeneous distribution of the reinforcement particles in the molten alloy. Stir casting was done in 1968 for first time for the aluminium MMCs by S. Ray [11] when he added alumina particles by stirring action in the molten aluminium. A general stir casting technique is shown in fig. 2 [6]. The main component in this method is the mechanical stirrer in the furnace. The casting of the resultant melt in the furnace containing ceramic reinforcements can be done by any of die casting, sand casting or permanent mold casting methods.

Stir casting is used for the production of composites with limited volume fraction of reinforcements which could be maximum 30% [7, 11]. Sometimes the final product have some porosity in it so after the casting the cast ingots are extruded for grain refinement and decreasing the porosity of composite and it also helps in homogenizing the reinforcement distribution. Segregation of the reinforced particles which can be caused due to surfacing and setting of the reinforced particles is the main concern in the casting process [13]. The final distribution of the reinforcement's in the cast product mainly depends on the material properties and processing parameters like the wetting condition of the reinforced particles with the melt, mixing speed, relative density, and rate of solidification.

Stir casting allows the utilization of standard metal processing methods with the help of suitable stirring system such as mechanical stirring, ultrasonic stirring, electromagnetic stirring, or centrifugal force stirring [6, 12]. Ultrasonic probe helps in breaking the agglomeration and clusters of the reinforcement particles formed in the matrix melt during the casting method so serving to the uniform distribution of the reinforced particles [11, 14]. The most important advantage of stir casting is its applicability to large quantity production. From all the known aluminium metal matrix composite fabrication ways, stir casting comes out to be the most economical and useful.

Ultrasonic vibration method is the most useful method for the purification, degassing of the molten alloy and also useful in the refinement of alloy melt in the furnace [12]. The ultrasonic fields in the liquid melt gives rise to non-linear effects such as cavitation and acoustic streaming. A general process of ultrasonic process is shown in fig. 3 below. The wettability is also improved between the matrix and reinforcement particles with the help of ultrasonic vibration. Work has been reported that particle reinforcement composite materials were produced with the help of ultrasonic field vibrations and also the reinforcement particles were mixed in the melts directly [14]. However, not much work has been reported on the in-situ synthesis of particle reinforcement MMCs with the help of ultrasonic assisted in-situ processing technique.

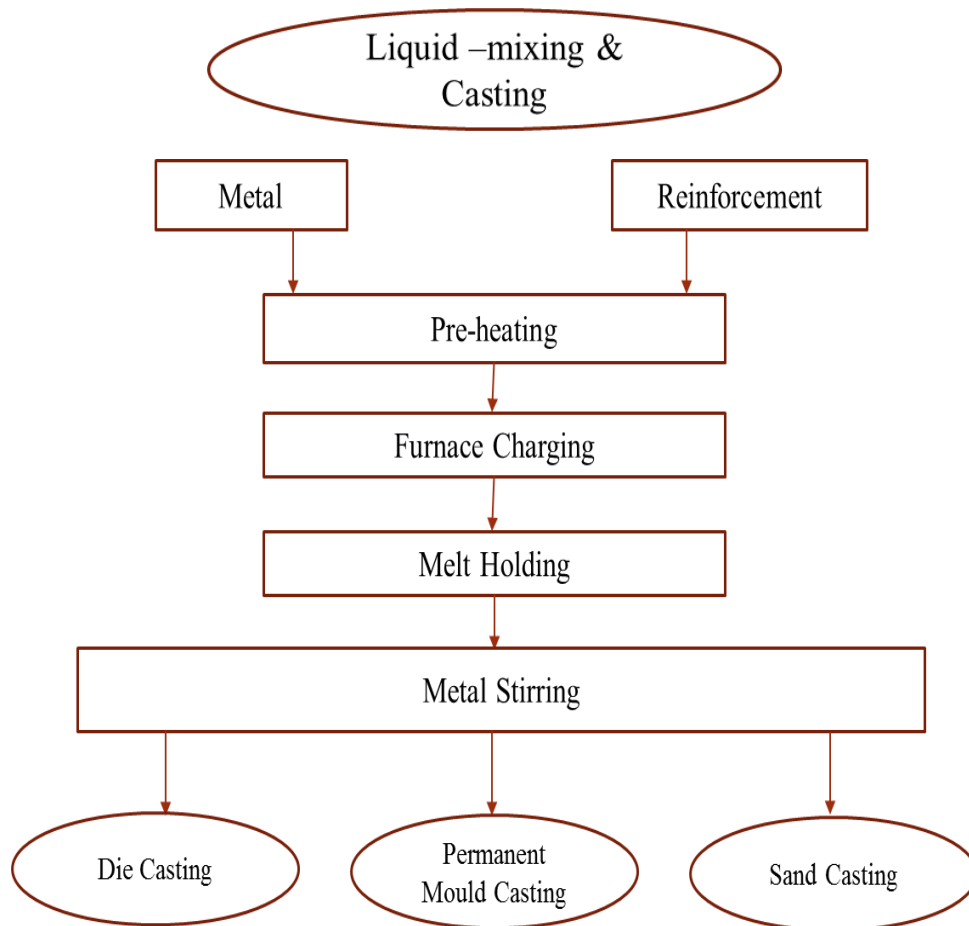


Fig. 2 Process of Stir Casting technique

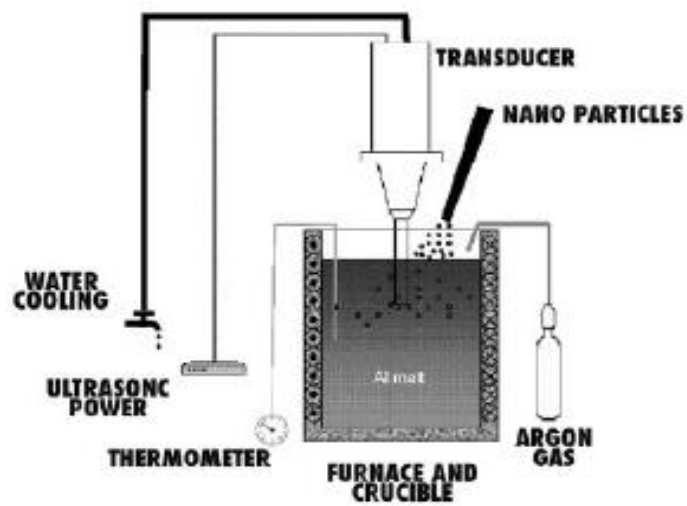


Fig. 3 Ultrasonic Assisted Casting Process [6].

2.4.2 In situ Synthesis of reinforcement particles

AMMCs with different reinforcements like TiC, SiC or TiB₂ can be produced by many techniques such as squeeze casting method, compo-casting method or powder metallurgy, etc. but all these processes for fabrication of composites are costly and require complicated equipment [12]. Therefore, in recent years a new route known as in-situ synthesis technique for the production of the composite is developed to reduce the cost of manufacturing. This technique gives us number of attractive features like uniform distribution of reinforcement particles, clear reinforcement/matrix interface and excellent compatibility between particles and matrix and also it is very cost effective method.

In-situ synthesis involves controlled metallurgical reactions of powdered salts for the production of reinforcement particles which is not the case in other manufacturing methods of composites [14]. In the reaction process while manufacturing a composite, one part is generally molten alloy and other part can be either of externally added fine powders or gaseous phases. Final product after the reactions is uniform distribution of the reinforcement particles in the matrix part of the final composite. These internally synthesized reinforcements thus have many desirable features. For example these particles are more coherent with the matrix material and has both finer particle size and a more uniform distribution. However, the method needs that the reaction system must be carefully screened. Typical method for in-situ synthesis process is shown in fig. 4.

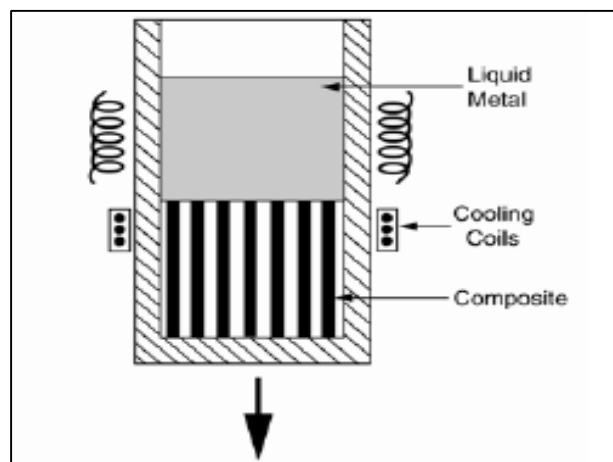
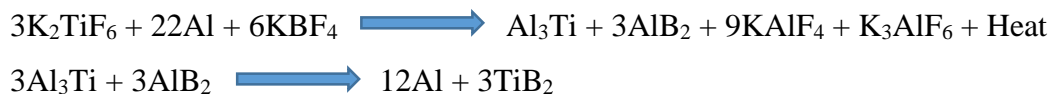


Fig. 4 Process of In-Situ synthesis [6]

Ref. [9] produced the Al-TiB₂ matrix composite which contains 12% by weight TiB₂ particles synthesized by in-situ salt metal reaction method. The produced Al-TiB₂ composite exhibited higher hardness values, also high strength and Young's modulus than the base matrix alloy. Ductility of the composite was observed to be slightly less than that of the Al 6061 alloy [9].

Formation of TiB₂ particles in in-situ processing of composites

In this process Al6061 base matrix alloy and halide salts that are potassium hexafluorotitanate (K₂TiF₆) and potassium tetra-fluoroborate (KBF₄) are used [14]. The halide salts are taken in the stoichiometric Ti:B ratio of 1:2. Further, the exothermic reactions between these salts yield in-situ formed TiB₂ particles in the alloy. As both salts are mixed stoichiometrically to form TiB₂, so it will be the only intermetallic phase to be formed by the reaction [11, 14]. The reaction scheme used to form the composite is given below:



2.5 Survey on Workability Studies of Aluminium MMCs

2.5.1 Workability and Processing Maps

Workability is defined as the extent till which a material can be deformed without any initiation of cracks in that material. Workability is a concept which depends on two factors that are material properties and the processing parameters [15]. Bulk deformation processes like extrusion, rolling and forging, etc. of materials are associated with the concept of workability.

Workability of any structural material is also governed by the ductility property of that material. Any material that have a good workability will have high ductility [15, 16]. But the two main important factors that are mostly considered for workability studies are: First is the material factor – which includes plasticity, grain size or microstructure, etc. and the second is process factor that includes the shape of that material, die geometry, etc.

Workability is also decided by some metallurgical factors such as grain size and distribution. Grain flow could be controlled in the forming methods which can improve the strength of the material in the possible loading direction. For example, in rolling process the grains orient themselves in a particular direction and thus provide directional variation in the properties also called as anisotropy. Also, it is known that coarse grained structure of the material decreases the workability of that material [16]. Cracks are also more liable to occur at the large grain boundaries. Therefore, to increase the workability hot working of materials is done. But there is a problem of grain coarsening associated with the hot forming. Titanium like materials are therefore added to help in forming of fine grained structure while doing the hot rolling process. It also helps in increasing the strength of that material [17].

Evaluation of the workability is done by using the processing maps. A processing map is basically used to identify or know the safe limits or regions for the forming processes and also it tells the crack formation regions or limits [16]. To draw the processing maps, process parameters such as strain rate, deformation temperature and strain rate sensitivity are used. From the processing maps, we can get to know the value of ductility of that material corresponding to a particular strain rate at a particular deformation temperature. A standard processing map is as shown in fig. 5.

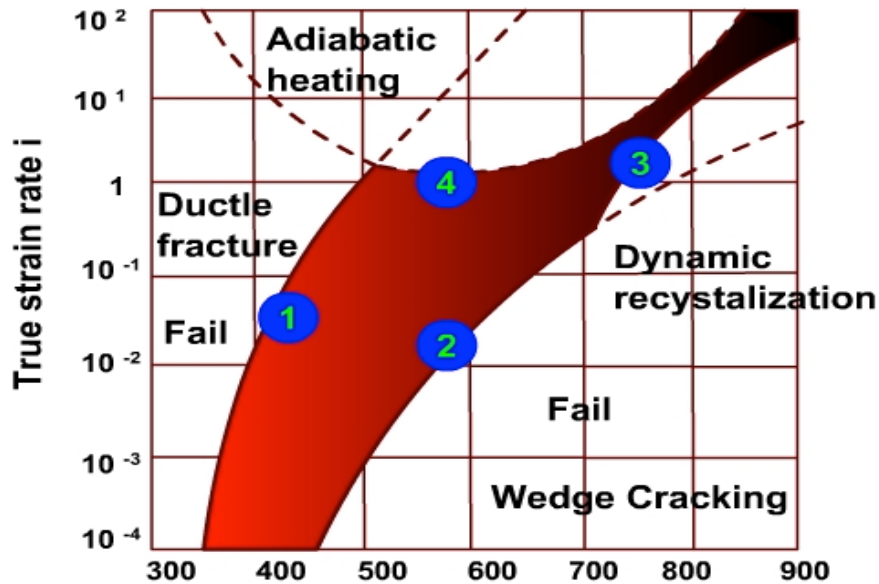


Fig. 5 Typical processing map. X-axis is temperature in degrees Celsius [16].

2.5.2 Metallurgical factors effecting workability

Workability is also contributed by some metallurgical factors such as strain hardening, texture, grain size, grain refinement, etc. as an example, we see that the crystallographic texture is promoted by the severe working of material and which ultimately results in anisotropy [17]. Due to the excessive working of any material, shear bands can also be generated because of the plastic instability during the compression.

Flow stress is then correlated with deformation temperature and strain rate in the dynamic material model at which the deformation is occurred. Form this one can easily map safe limits of hot working of that material and also the fracture limits under the varying deformation temperatures and strain rate conditions can be mapped. Two very important parameters considered in this technique are strain rate sensitivity and the deformation temperature of hot working [18]. The DMM integrates the flow stress, temperature, and microstructure, with the workability.

The parameter m , is known as strain rate sensitivity. The equation as follows gives the value of m [19]:

$$m = \left. \frac{\partial \log \sigma}{\partial \log \dot{\epsilon}} \right|_{\epsilon, T}$$

2.5.3 Dynamic recovery and Dynamic recrystallization Phenomena

Effect of strain rate on the flow stress is more pronounced in hot working conditions. Hot working significantly increases the workability of material [16]. Throughout hot working, the phenomena of dynamic recovery and recrystallization contributes to softening of the materials. Typical plot of dynamic recovery and recrystallization is shown in fig. 6 below. Dynamic recovery involves the dislocation cross slip, and annihilation of dislocations, and thereby forming the sub grains. As a result the flow stress is reduced. Uniform equiaxed grains form as a results of dynamic recovery.

Dynamic recrystallization tends to occur in materials that have high stacking fault energy. When the dislocation density will increase to higher levels, recrystallization is the only chance through which the inner strains can get relieved. High dislocation density and recrystallization may lead to internal cracks during forming.

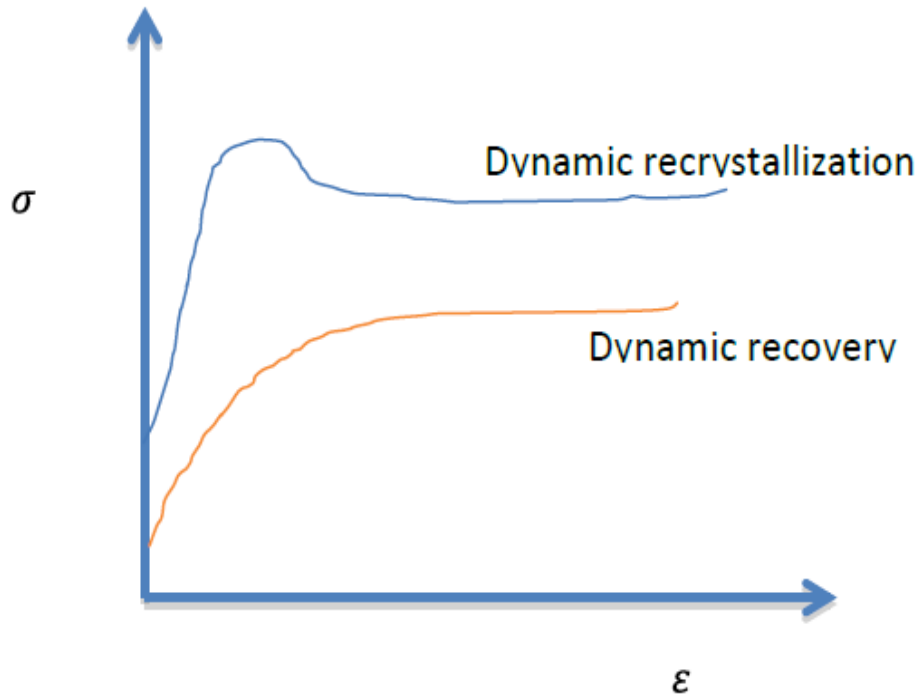
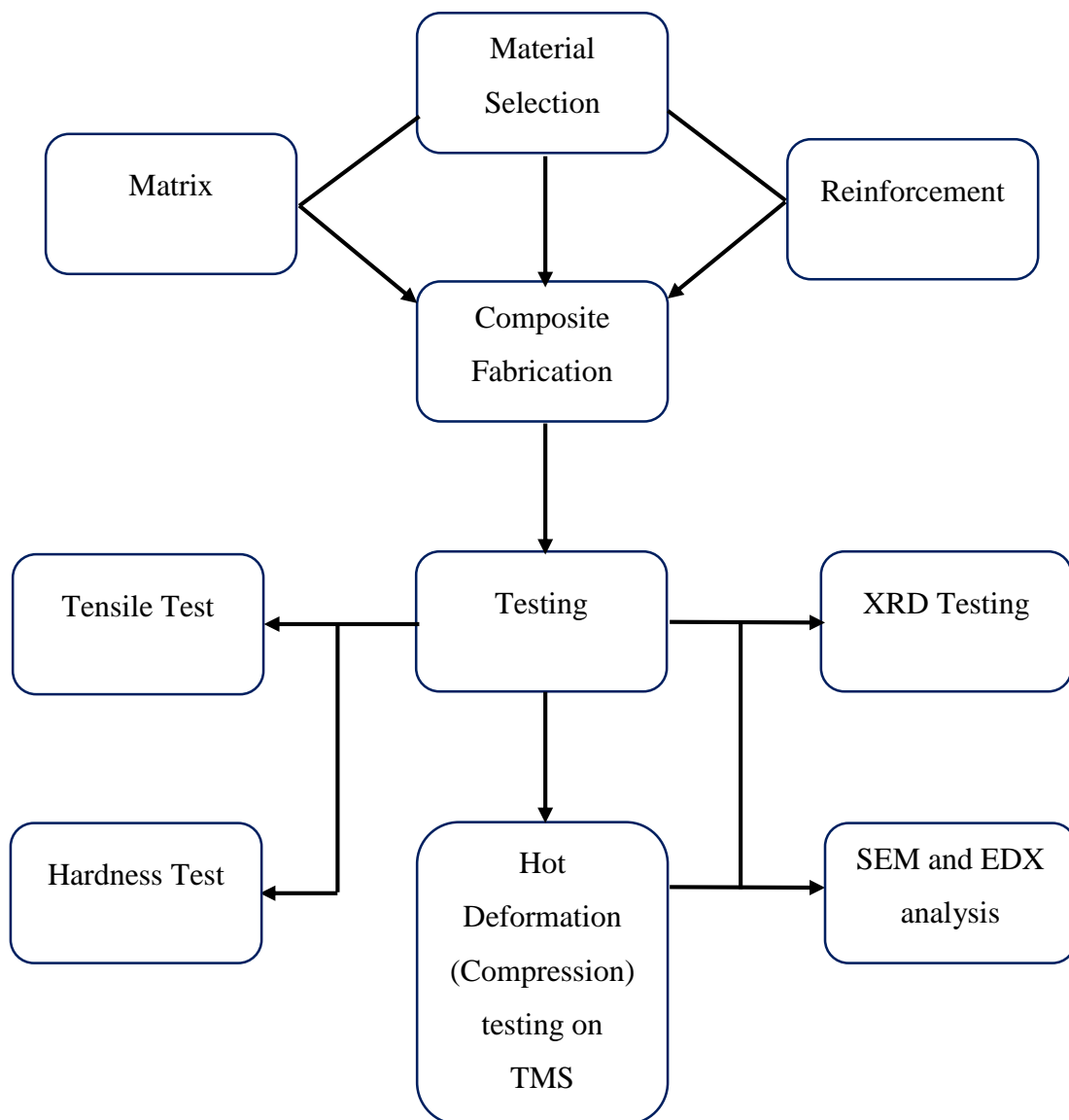


Fig. 6 Typical Plot of Dynamic recovery and recrystallization.

It is seen that the workability of cast materials like composite materials is generally not that good so these are usually hot worked so as to improve their workability to some extent [19]. Low melting point phases that are present in any material can be the cause of localized melting which will further cause hot shortness. Material gets strain hardened or work hardened during the cold working and the stresses in that material does not get relieved. So, as a result the workability of that material is decreased. Whereas hot working conditions increases the workability as dynamic recovery phenomena is involved in the case of hot working of any material.

Experimental research has been performed to check the workability of MMCs reinforced with SiC and Al₂O₃ using the up-set tests [20]. Aluminium MMCs were prepared by completely different techniques, stir casting, squeeze casting and powder metallurgy. Stir casting resulted in a slightly higher workability than that obtained in the case of powder metallurgy, whereas squeeze casting showed promising behavior within the case of composites with high-particulate volume fraction [16]. Also, it had been reported that localized shear flow of the matrix might control the failure of the composite under compression [20, 22].

Plan of work is easy to understand in a flow chart form. So, flow chart is drawn to show my work plan which includes material selection followed by the composite fabrication. Then comes the testing work which includes mechanical and microstructural testing. Mechanical testing includes tensile test, Vickers hardness test and hot deformation tests whereas microstructural testing includes XRD, SEM and EDX analysis.



4.1 Material Selection

- **Matrix** : Al 6061 alloy

Chemical composition of Al 6061[7]

Element	Mg	Si	Fe	Cu	V	Mn	Ti	Al
Weight %	1.08	0.63	0.17	0.32	0.01	0.52	0.02	Remainder

- **Reinforcement**

TiB₂ reinforcement is synthesized by in-situ processing method in which Titanium (K₂TiF₆) and Boron (KBF₄) salts taken in a stoichiometric Ti:B ratio of 1:2 are added in the alloy matrix.

4.2 Fabrication of Al-TiB₂ Composite

Aluminum composites with TiB₂ reinforcement (9%, 3%, and 5% by weight) in Al6061 matrix were manufactured by the in-situ processing technique which involves the salt-metal reaction between the titanium salt K₂TiF₆ and the boron salt KBF₄. From all the produced composites, the one with 5% by weight reinforcement was successfully manufactured and then further used for mechanical testing and workability testing on thermo mechanical simulator. The casting product was produced by ultrasonic assisted stir casting route. Furnace used for fabrication of composite is shown in fig. 7 below.

1. Al6061/TiB₂ (9wt.%) composite

First of all, 360 grams of Al 6061 alloy was taken in the graphite crucible and then heated in an electrical furnace for melting. Temperature of furnace was maintained at 800 °C which will be reaction temperature for the salts to be added. Now, titanium (K₂TiF₆) salt and boron (KBF₄) salts were taken in stoichiometric ratio of 1:2, mixed properly and kept in an oven for preheating at 200 °C. After approximately 2.5 hours, temperature of the furnace reached to 800 °C and molten alloy was ready. Then the

preheated mixture of salts was added into the molten alloy in the furnace. Manual stirring was done for about 10 minutes to mix the salts in the melt. Further, melt was kept for reaction time of 60 minutes at the same 800 °C temperature to get the required reinforcement product from the reaction of salts. After completion of reaction, the reaction slag was skimmed out from the surface of the melt and molten material is poured from crucible to the metal mould and kept to solidify under normal air conditions. After solidification cast ingot was taken out of the metal mould and taken for further experimentation work.

2. Al6061/TiB₂ (3 wt.%) composite (Ultrasonic assisted)

First of all, 350 grams of Al 6061 alloy was taken in the graphite crucible and then heated in an electrical furnace for melting. Temperature of furnace was maintained at 850 °C. Now Titanium containing K₂TiF₆ salt and Boron containing KBF₄ salt were taken in stoichiometric ratio of 1:2, mixed properly and kept in an oven for preheating at 200 °C. After approximately 2 hours, temperature of the furnace reached to 850 °C and molten alloy was ready. Then the preheated mixture of halide salts was added into the molten alloy in the furnace. Manual stirring was done for 10 minutes to mix the salts in the melt. Further, melt was kept for reaction time of 30 minutes at the same 850 °C temperature to get the required reinforcement product from the reaction of salts. After 30 minutes of reaction time, ultrasonic stirring was done by **Ti-Al-V alloy rod** (coated with Zirconia) for 5 minutes to take care of any clustering and agglomeration of particles formed by the reaction of titanium and boron salts. Then, the reaction slag was skimmed from the surface of the melt and molten material is poured from crucible to the metal mould and kept to solidify naturally under normal air conditions. After solidification cast ingot was taken out of the metal mould and taken for further experimentation work.

3. Al6061/TiB₂ (5 wt.%) composite (Ultrasonic assisted)

First of all, 380 grams of Al 6061 alloy was taken in the graphite crucible and then heated in an electrical furnace for melting. Temperature of furnace was maintained at

850 °C. Now titanium containing K_2TiF_6 salt and boron containing KBF_4 salt were taken in stoichiometric ratio of 1:2, mixed properly and kept in an oven for preheating at 200 °C. After approximately 2.5 hours, temperature of the furnace reached 850 °C and molten alloy was ready. Then the preheated mixture of halide salts was added into the molten alloy in the furnace. Manual stirring was done for 10 minutes to mix the salts in the melt. Further, the melt was kept for reaction time of 30 minutes at the same 850 °C temperature to get the required reinforcement product from the reaction of salts. After 30 minutes of reaction time, ultrasonic stirring was done by **Ti-Al-V alloy rod** (coated with Zirconia) for 10 minutes to take care of any clustering and agglomeration of particles formed by the reaction of titanium and boron salts. Then, the reaction slag was skimmed from the surface of the melt and molten material is poured from crucible to the metal mould and kept to solidify naturally under normal air conditions. After solidification cast ingot was taken out of the metal mould and taken for further experimentation work.



Fig. 7 Furnace used for the casting of in-situ Al composites.

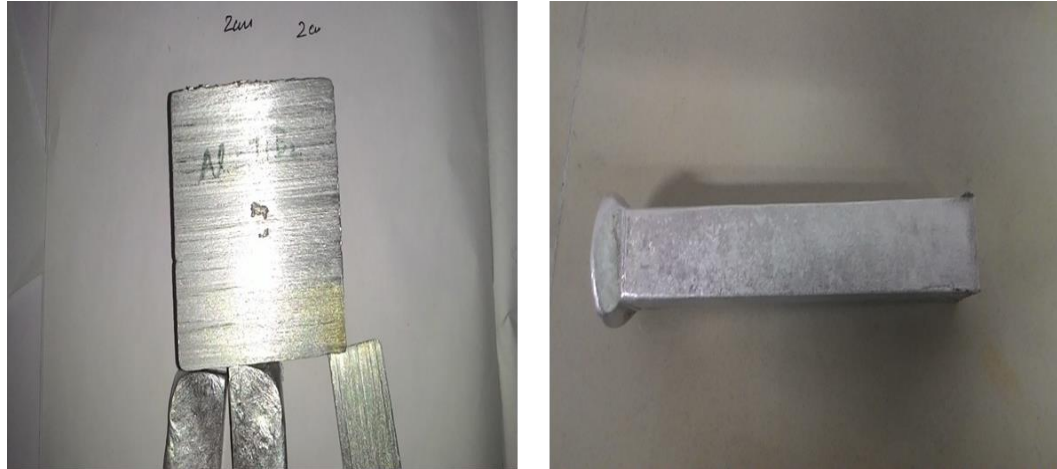


Fig. 8 Cast ingots of the composites manufactured in MMED department of IIT Roorkee

4.3 Tensile Test

Standard ASTM E8 dimensions are used for making the samples. Samples have round cross-section with plane shoulders and samples are prepared from all the castings. Tensile testing was then done on all the samples and readings are reported in the results and discussions.

The dimensions of tensile specimen is also given in the table 2 below. Typical diagram with the standard dimensions for the tensile specimen is shown in fig. 9 as follows and fig. 10 shows the universal testing machine.

Table 2 Standard Dimensions of Tensile Samples

Gauge diameter	4 mm
Gauge length	20 mm
Length of grip section	8 mm
Overall length	36 mm

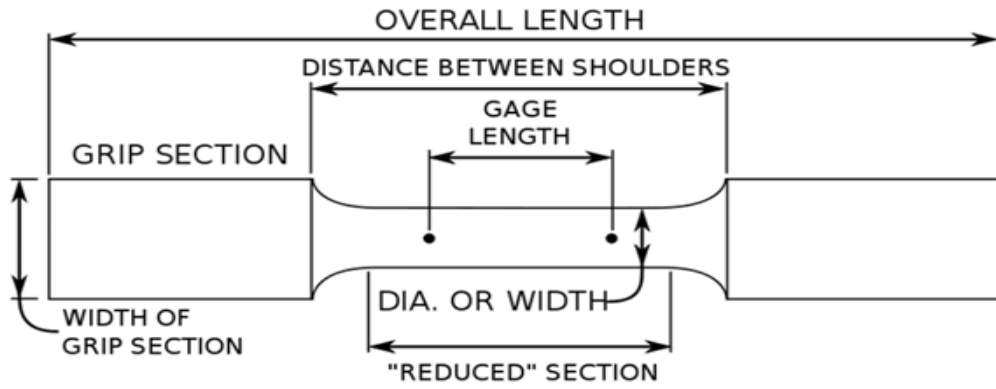


Fig. 9 Schematic diagram of a Tensile Sample



Fig. 10 Universal Testing Machine Model H-75 KS for tensile testing

4.4 Vickers Hardness Test

The ability of a material to resist the plastic deformation from a standard source is known from the hardness measurement of the material. One of the widest scale in hardness testing comes in the Vickers hardness testing of almost all the metals. Diamond pyramid number or Vickers hardness number (HV) is used as the unit of hardness. The hardness number can also be converted into units of Pascal, but should not be confused with a pressure, which also has units of Pascal.

Vickers tester machine is shown below in fig. 11.

- Cylindrical samples from the composites and alloy were made and prepared for the hardness test. For this test, the surface of the material should be plane and scratch free so the samples were polished on emery paper and cloth to get the required surface. Firstly, the samples were polished on emery paper (Silicon carbide waterproof paper) of different grades that are 320, 800, 1200 and 1500 and then finally cloth polished.
- After the samples are ready, they were taken for the test and five indentation readings were taken for each sample at different locations and then averaged to get the hardness value of the material. The indenter used for these measurements was diamond indenter.



Fig. 11 Computerized Vickers Hardness Tester in MMED, IIT Roorkee

4.5 Scanning Electron Microscopy (SEM)

Reinforcement distribution in the matrix of the composite is examined by microstructural characterization studies. This is done most effectively with the help of SEM analysis. Samples from all the castings of different composites were prepared and SEM images were taken initially before any hot deformation (compression) testing and also taken after the hot deformation testing. After the hot deformation testing, the samples were cut parallel to the compression axis and the sectioned planes were prepared by standard polishing techniques for the SEM analysis. For all samples we have to first prepare them by standard metallographic polishing techniques for SEM examination. Standard polishing techniques includes polishing on the emery paper followed by fine grain clothe polishing. Secondary electron mode is used for obtaining the SEM images. Scanning electron microscope is also equipped with EDX detector of Oxford data system. EDX was also performed on the prepared samples for the confirmation of reinforcement presence in the composite material. Scanning electron microscopy facility in MMED, IIT Roorkee is shown in fig. 12 below.



Fig. 12 Scanning Electron Microscopy facility in MMED, IIT Roorkee

4.6 X-Ray Diffraction (XRD) Analysis

XRD analysis is basically done to determine which phases are there in the manufactured composite material. Either of bulk or powdered samples can be used for the XRD testing. It gives the intensity vs. degree plot which shows the intensities of all the different phases present in the composite material. Mostly, bulk samples are used in the XRD analysis but wherever the phase is present in small amount, powdered sample is prepared and examined.

For powder sample, we have to first prepare the powder samples by Leaching (Extraction) process shown in fig. 13 below which involves:

- Firstly, composite samples were filed and powdered samples were collected.
- Powdered samples are then leached in HCl (20% v/v) solution for 5-6 days.
- Leached powder is then collected, washed, dried and sent for XRD.



Fig. 13 Extraction process for XRD sample preparation

4.7 Hot Compression tests on TMS

Gleeble 3800 thermo mechanical simulator in MMED, IIT Roorkee was used for the uniaxial hot deformation (compression) testing [16]. Strain rate was kept in the range from 0.001 to 0.1 s⁻¹ with four different temperatures ranging from 300 °C to 450 °C. Cylindrical samples were made for hot deformation (compression) testing with dimensions of diameter 10 mm and height 15 mm [19]. Load-stroke data has been used for obtaining the flow stress data. Chromel/Alumel thermocouple was also welded at the center of the height of sample to monitor the temperature of the sample as stated by Prasad and Rao [18]. Adiabatic temperature increment is also studied with the help of thermocouple in the sample throughout the deformation (compression) process.

Deformed friction is effectively reduced with the help of graphite lubrication and the samples were effectively deformed to 0.6 true strain. Samples were deformed to half the original height of the samples. Water quenching is also done just after the completion of hot compression testing. After the testing, all samples were cut parallel to the compression axis and the cross-sectioned planes were prepared by standard techniques and sent for microstructure analysis by SEM. The SEM images obtained at different magnifications for different strain rate conditions with all four temperatures are then reported in the results and discussions part.

Determination of deformation parameters of the material and Creation of Processing Maps:

The deformation behavior is generally governed by the strain hardening effect and also the inner constitution of any composite material. Increasing strain rate in the hot processing also increases the strength of any composite material.

Equation (1) given below gives us the rate sensitive flow behavior [16, 17].

$$\sigma = K\dot{\epsilon}^m \quad \text{Eq. (1)}$$

Where, K is a parameter and it depends on the structure of the material and also on the temperature. 'm' is known as the strain rate sensitivity parameter. The value of m is calculated by the following equation (2) given at a constant strain and temperature [17].

$$m = \left. \frac{\partial \log \sigma}{\partial \log \dot{\epsilon}} \right|_{\epsilon, T} \quad \text{Eq. (2)}$$

The complexity of dynamic processes also influences the deformation behavior of any composite material [17]. Generally, two power dissipation routes accompany hot deformation (compression) processes: (1) power which will be required to bring the microstructural changes in the composite material, (2) dissipation in the heat generation throughout the hot deformation. The flow obtained is generally proportional to the strain rate in an ideal condition at any temperature and strain. Ratio of dissipated heat in microstructural changes to the max heat dissipation is called the efficiency of hot deformation. The following equation (3) below gives the efficiency [15, 16]:

$$\eta = 2m / m + 1 \quad \text{Eq. (3)}$$

Where, m is known as strain rate sensitivity parameter of any material. It is a function of strain rate and the temperature of processing. Processing map for any hot deformed material is constituted by the iso-efficiency contours on temperature-strain rate plots/graphs. Efficiency contours thus help for identifying different domains or regions on the processing maps. Dominant deformation mechanism is represented by each of them. Optimum hot deformation conditions have the peak efficiency in all the domains on the map. Instability criterion in addition to efficiency contours is given by following equation (4) [18, 22]:

$$\xi(\dot{\epsilon}) = \left\{ \delta \ln \left[\frac{m}{m+1} \right] / \delta \ln(\dot{\epsilon}) \right\} + m < 0 \quad \text{Eq. (4)}$$



Fig. 14 Gleeble-3800 thermo mechanical-simulation facility in Materials and Metallurgy department, IIT Roorkee

5.1 Tensile Test Results

Tensile tests were done on TiB_2 composite samples of standard dimensions from all the cast ingots and the averaged values are tabulated in table 3. Properties and nature of reinforcements and matrix material are important functions which influences the tensile properties of composite materials. The reason of the development in tensile property of the TiB_2 composite is the contact between TiB_2 particles and the dislocations. TiB_2 reinforcement particles act as barriers to the dislocation movement when the composite is under load, and thus enhances the tensile strength of composite. The efficient transfer of the load from the matrix to the TiB_2 reinforcements is facilitated by the uniformly distributed particles along with the clear interface between matrix and reinforced particles. Thus, stress needed for the formation of cracks at the interface is increased [12]. Stress-Strain graphs are shown in fig. 15 below.

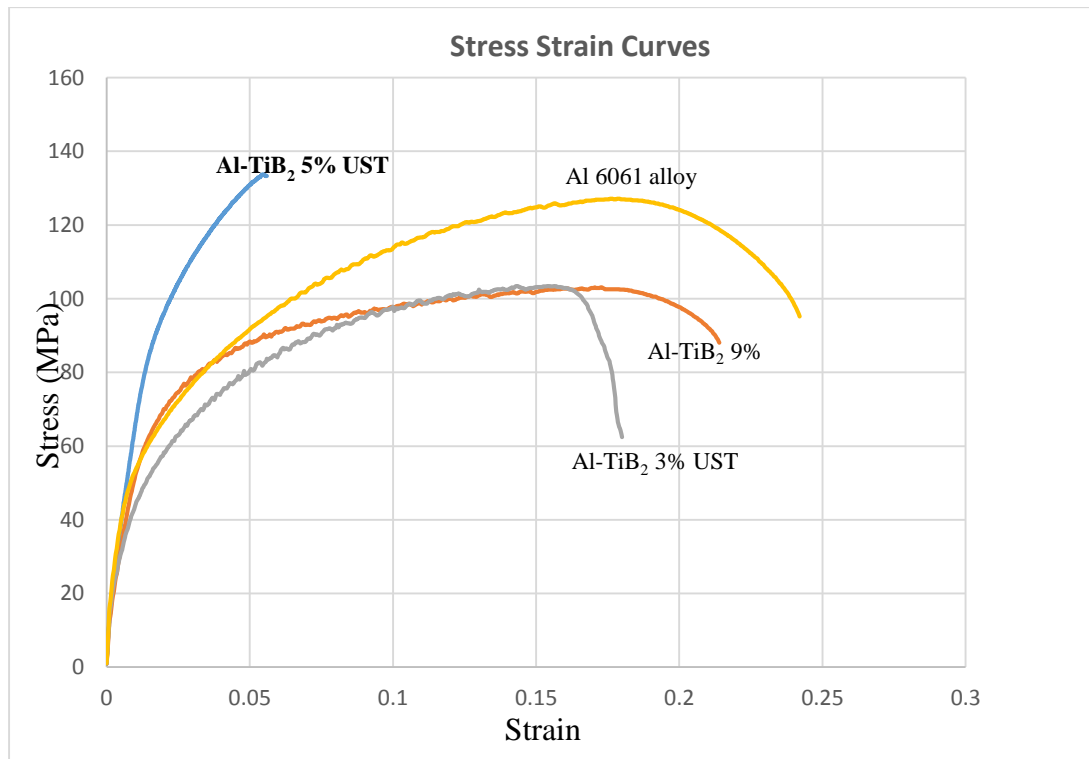


Fig. 15 Stress-strain plots

Table 3 Stress-Strain Values for the composites

Specimen	Yield Stress (MPa)	Max Stress (MPa)	Ext. @ break
Al6061 as cast	56.7	127.1	0.242
Al-TiB₂ – 9 wt.%	48.1	99.35	0.195
Al-TiB₂ – 3 wt.% UST	50.99	103.4	0.18
Al-TiB₂ – 5 wt.% UST	59.23	134.1	0.071

5.2 Hardness Measurement

Table 4 is showing the results obtained from hardness testing of Al 6061 alloy and its in-situ composites. It is experimentally known that the hardness of any composite will increase with the incorporation of hard reinforcements like TiB₂ into the ductile or soft matrix materials [7]. As TiB₂ is a hard reinforcement, it will give its inherent property of hardness to the matrix material, and therefore increases its resistance to deformation [9]. Grain refinement and fine grains of the matrix material along with the reinforcement used also influences the hardness behaviour of the composite material.

It is also known that the fabrication techniques and quality of the casting produced also greatly influences the increment in hardness value of that composite [11]. A very interesting factor that affects the hardness value of any composite material is the extent of bonding between reinforcement particles and the matrix material.

Table 4 Hardness values

Specimen	Vickers Hardness (at 1 kgf)
Al6061 as cast	50.2 HV
Al-TiB₂ – 9 wt.%	34.7 HV
Al-TiB₂ – 3 wt.% UST	41.05 HV
Al-TiB₂ – 5 wt.% UST	55.1 HV

5.3 X-Ray Diffraction Analysis (XRD)

The X-Ray diffraction patterns of the manufactured composites are shown in the given figures. X-Ray patterns shows us that the composite is consisted of TiB_2 reinforcement particles with some traces of Al_3Ti and TiB particles also in 9 wt. % composite. Since both the halide salts, K_2TiF_6 and KBF_4 were mixed in the ratio of 1:2 to form TiB_2 reinforcement, TiB_2 is the main intermetallic product formed by the metallurgical reactions in the melt and this is also confirmed by the XRD analysis. Fig. 16 shows the XRD pattern of 9 wt. % TiB_2 composite which also have some traces of Al_3Ti . Fig. 17 and 18 shows the XRD patterns of 3 and 5 wt. % composites respectively.

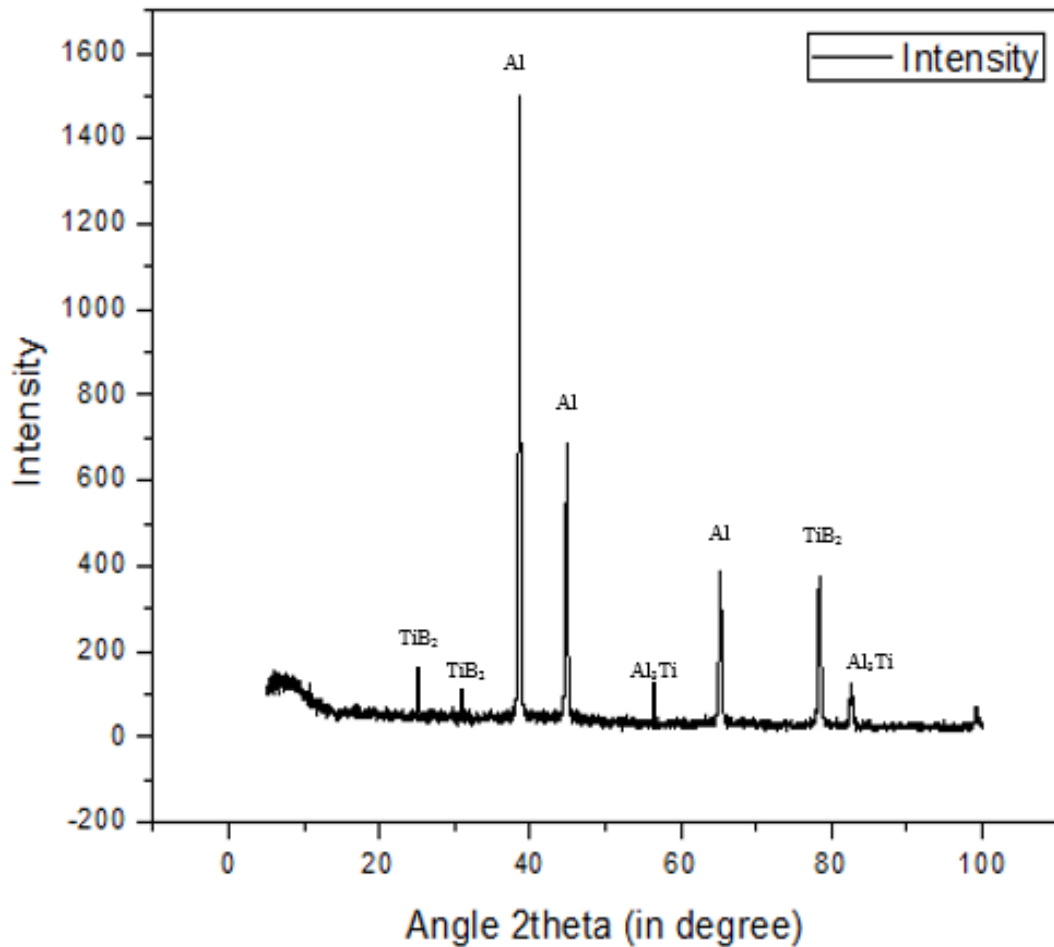


Fig. 16 XRD patterns of in situ 9 wt. % Al- TiB_2 composite

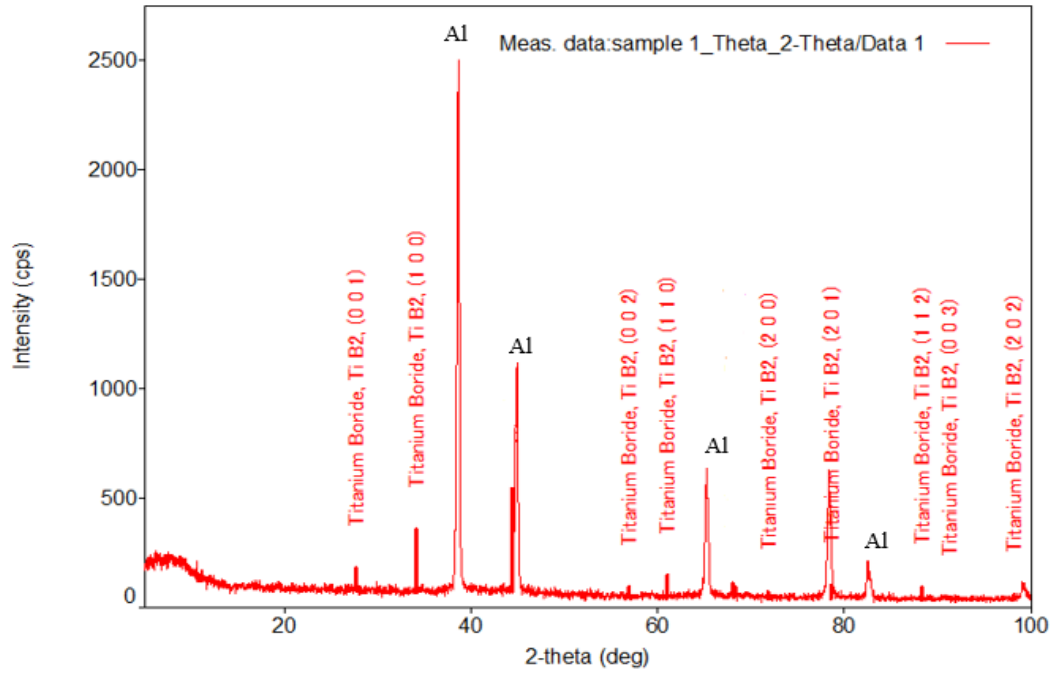


Fig. 17 XRD patterns of in-situ 3 wt. % Al-TiB₂ composite fabricated by Ultrasonic assisted technique

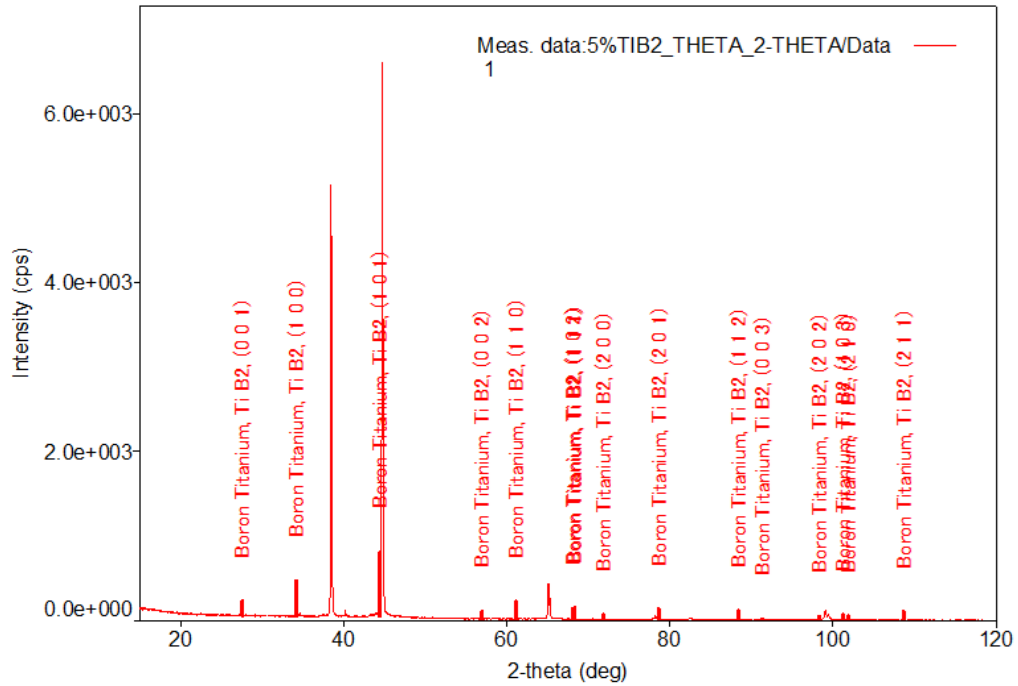


Fig. 18 XRD patterns of in-situ 5 wt. % Al-TiB₂ composite fabricated by Ultrasonic assisted technique

5.4 SEM Images of the manufactured Al-TiB₂ composite:

SEM images of the manufactured composites before the hot deformation testing were obtained and shown in the figures below. Sample were made from all the castings and prepared by standard metallographic techniques for SEM examination. Results shows the distribution of the reinforcement particles in the matrix. Confirmation for the presence of reinforcement particles in the composite was done with the help of EDX analysis. Fig. 19 and 20 shows the SEM images and EDX analysis.

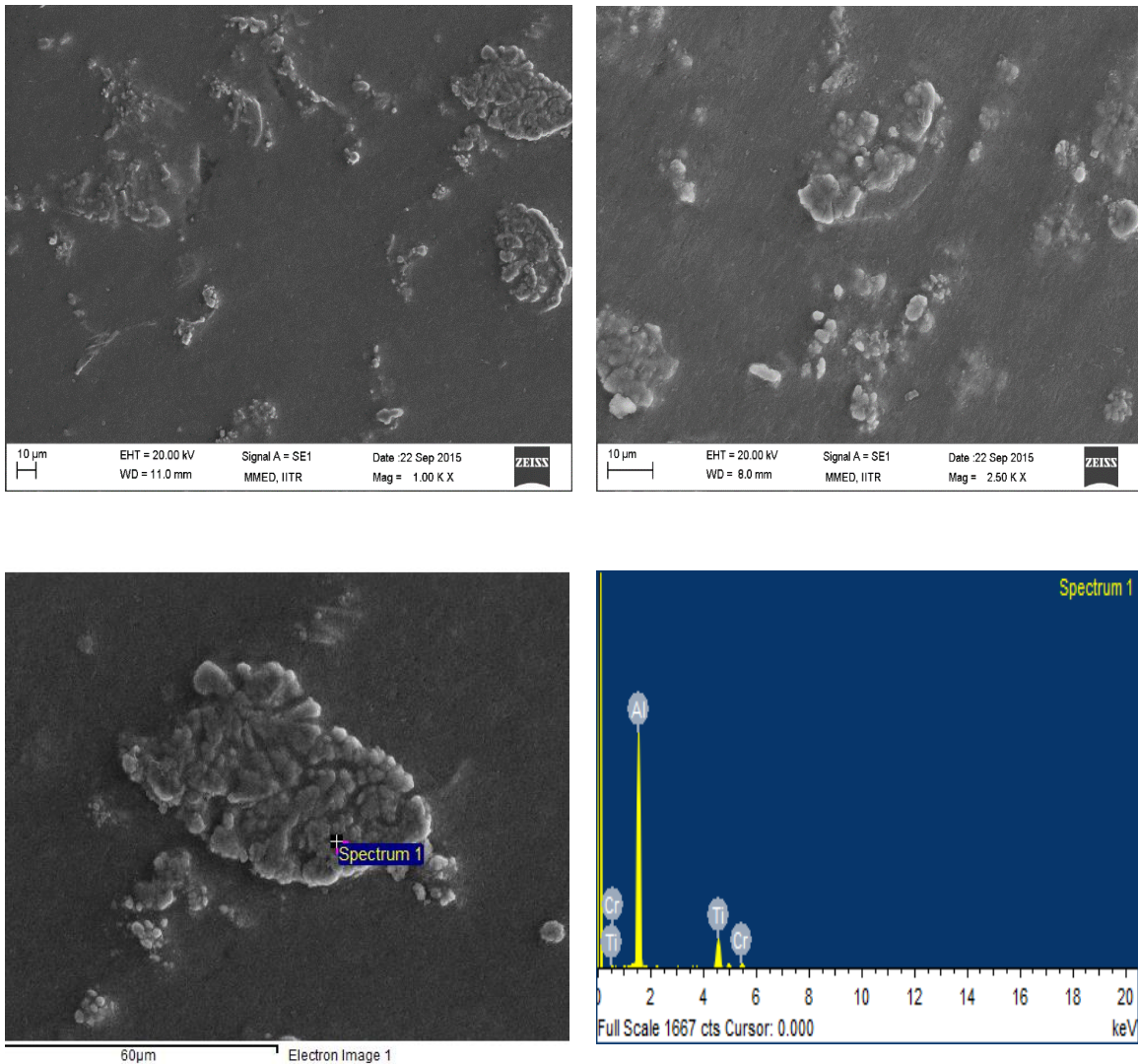
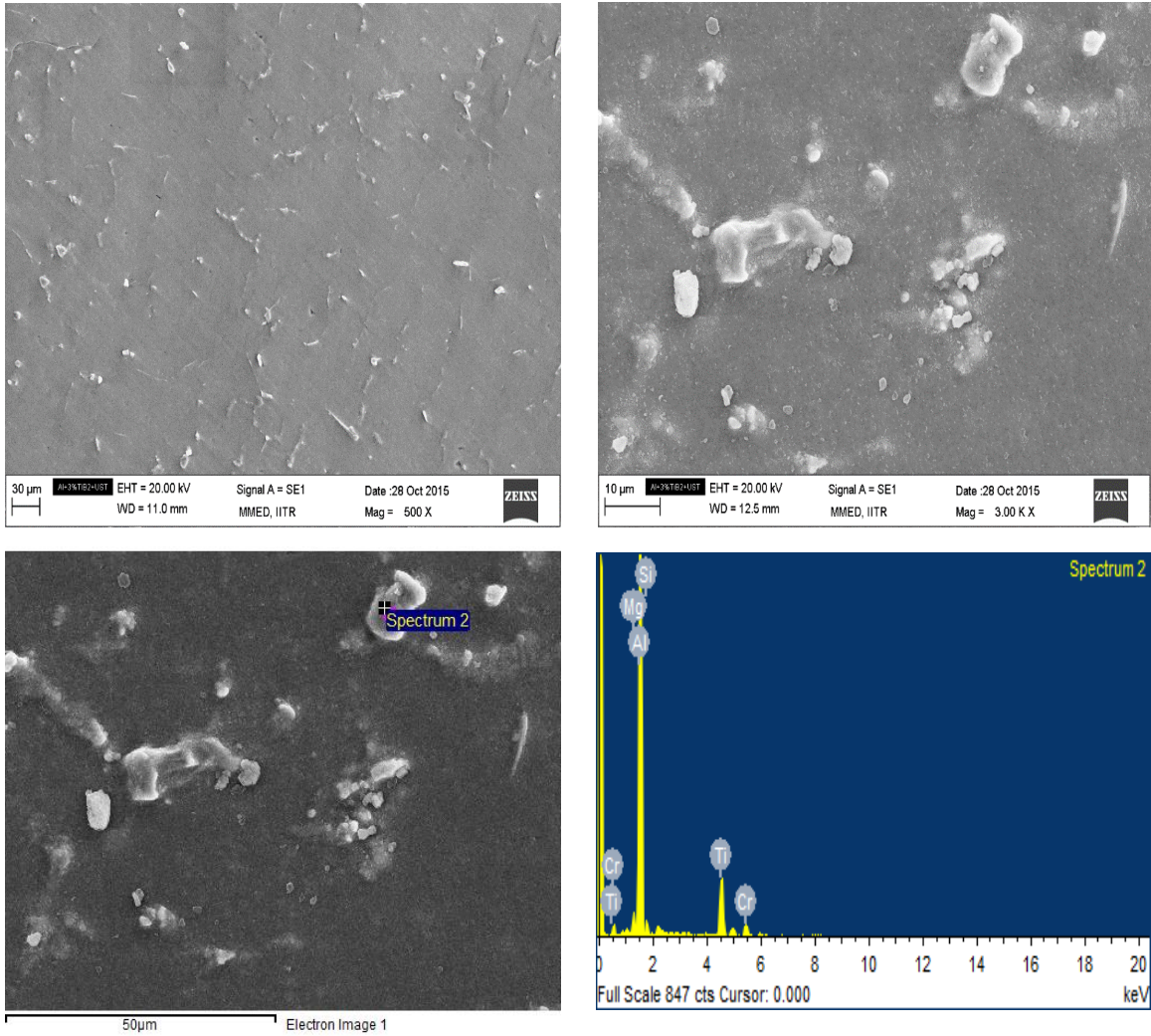


Fig. 19 SEM images and EDX analysis of produced Al6061/TiB₂ composite (9% by weight).



Element	Weight%	Atomic%
Mg K	1.70	2.12
Al K	70.19	78.94
Si K	3.16	3.41
Ti K	19.51	12.36
Cr K	5.44	3.18
Totals	100.00	

Fig. 20 SEM images and EDX analysis of Al6061/TiB₂ composite formed by ultrasonic assisted technique (5% by weight).

5.5 Hot Compression Testing on TMS

5.5.1 True Stress-Strain Behavior

True stress-true strain graphs at the constant initial strain rates, ranging from 0.001 s^{-1} to 1 s^{-1} , and constant temperatures over the range of $300 \text{ }^{\circ}\text{C}$ to $450 \text{ }^{\circ}\text{C}$ are shown in fig. 21 and 22. The strain rate and temperature both significantly influences the flow stress. In a typical true stress-true strain curve, the flow stress rapidly increase at first, and then experiences slow increase to reach a plateau consequently. Usually in the hot compressive deformation method, the increase in the flow stress is due to the strain hardening. The balance between the strain hardening and softening results in the steady state in flow stress curves. The strain softening is thus taken into account caused by the dynamic recovery or dynamic recrystallization within the composite material [17, 18].

The true stress-true strain graphs shows us that with the increasing strain rate, the flow stress also increases along with the decreasing hot deformation temperature. Also the dispersive hardening effect of the TiB_2 reinforcement particles has increased the strength of the composite.

The number of dislocations formed and their movement rate is also increased with the increasing strain rate. Also, at same time softening rate is decreased because of the decrease in climbing and reaction rate of dislocations generated. As the work hardening is severe, critical shear stress will also increase. But, with increasing hot deformation temperature, heat activation energy also increases and decreases the critical shear stress. Thereby improving the softening effect which is caused by dynamic recrystallization.

Dynamic recovery involves the dislocation cross slip, and annihilation of dislocations, and thereby forming the sub grains. As a result the flow stress is reduced. Uniform equiaxed grains form as a results of dynamic recovery. Dynamic recrystallization tends to occur in materials that have high stacking fault energy. When the dislocation density will increase to higher levels, recrystallization is the only chance through which the inner strains can get relieved. High dislocation density and recrystallization may lead to internal cracks during forming.

➤ At Constant Strain rates:

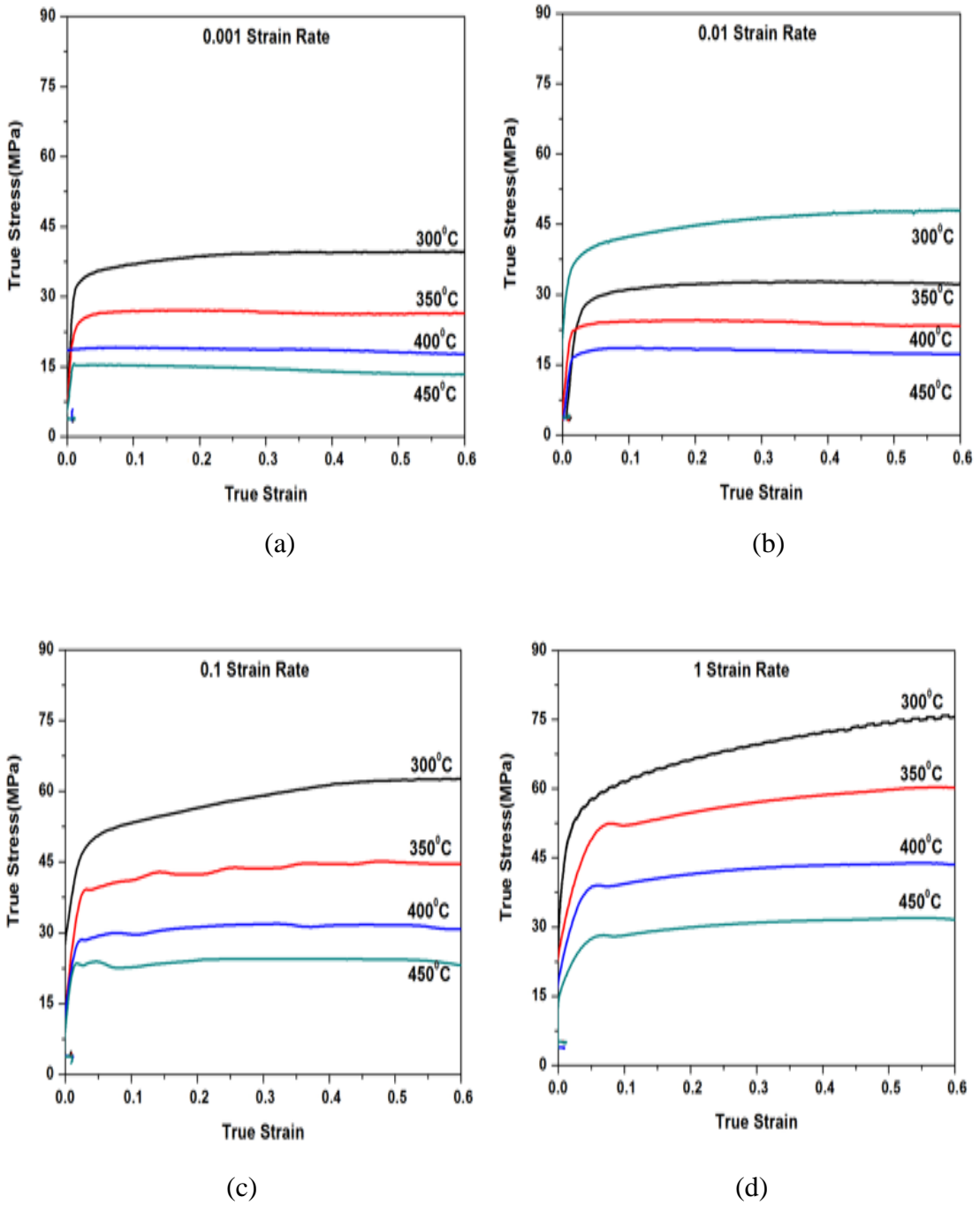


Fig. 21 True stress-true strain plots at strain rates (**0.001 s⁻¹ to 1 s⁻¹**): (a) 0.001 s⁻¹; (b) 0.01 s⁻¹; (c) 0.1 s⁻¹; (d) 1 s⁻¹ and at 300 °C, 350 °C, 400 °C, and 450 °C .

➤ At Constant Temperatures:

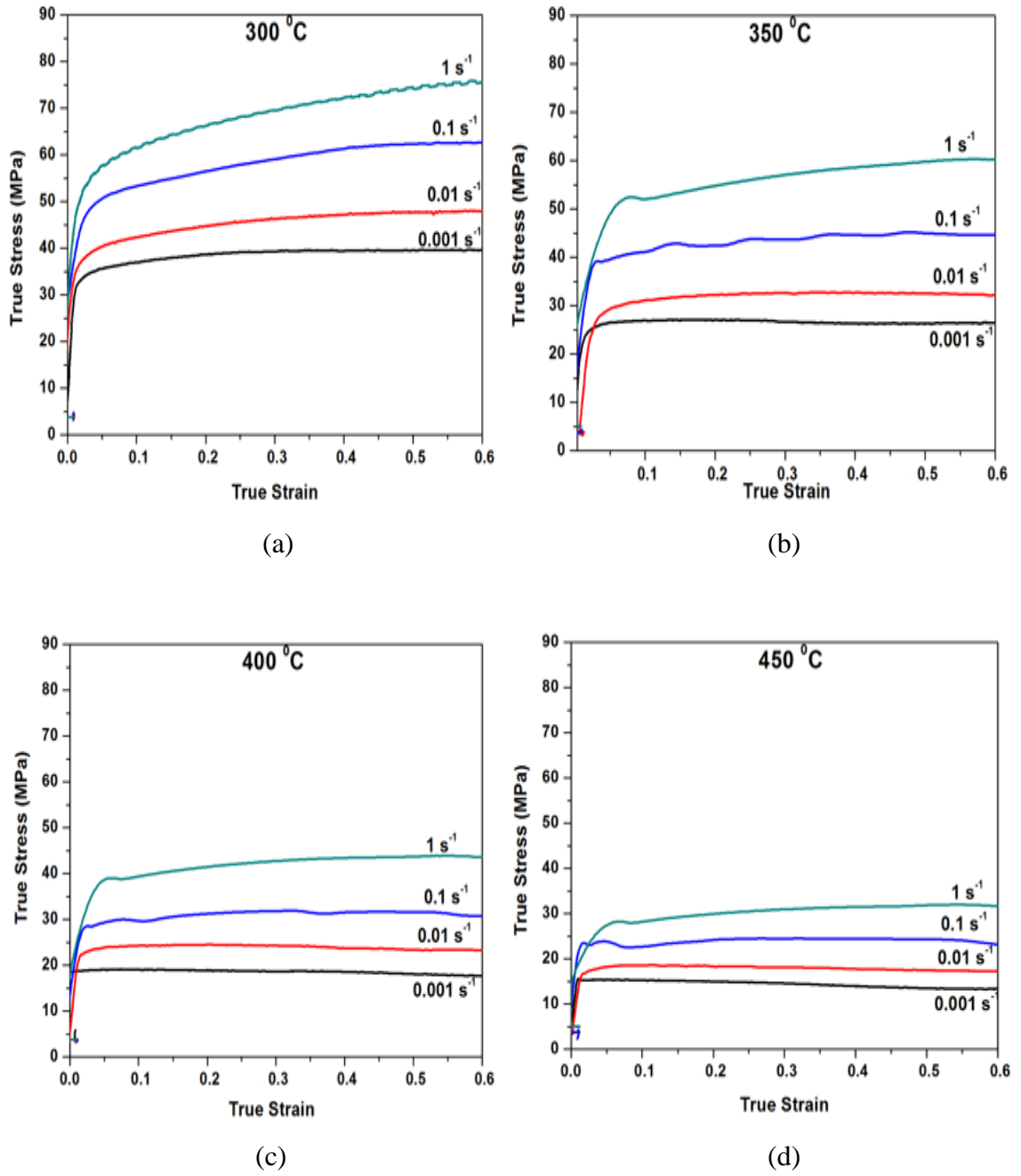


Fig. 22 True stress-true strain plots at constant temperatures (300 °C to 450 °C): (a) 300 °C; (b) 350 °C; (c) 400 °C; (d) 450 °C.

5.5.2 Constitutive Equation for the deformation of the composite

Fig. 21 and 22 shows the compressive stress-strain curves of the deformed composite. The strain rate and the temperature each have the significant influence on the flow stress. In the hot deformation, the dependence of the temperature and strain rate on the flow stress is expressed by Zener-Hollomon parameter (Z) in an exponent form as follows [20, 21]:

$$Z = \dot{\epsilon} \exp\left(\frac{Q}{RT}\right) \quad \text{Eqn. (1)}$$

Where, $\dot{\epsilon}$ is the strain rate (s^{-1}),

R is the gas constant ($8.3145 \text{ Jmol}^{-1}\text{K}^{-1}$),

Q is the activation energy of hot deformation (kJ/mol),

T is the temperature (K).

The Zener-Hollomon parameter (Z) can be represented in different stress divisions:

- For low stress level ($\alpha\sigma < 0.8$), the power law is used.
- For high stress ($\alpha\sigma > 1.2$), the exponential law is adopted.
- For all level of stress, the hyperbolic law in Arrhenius type equation has the best results between Zener-Hollomon parameter and stress.

$$Z = \dot{\epsilon} \exp\left(\frac{Q}{RT}\right) = A\sigma^{n'} \quad \alpha\sigma < 0.8 \quad \text{Eqn. (2)}$$

$$Z = \dot{\epsilon} \exp\left(\frac{Q}{RT}\right) = A \exp(\beta\sigma) \quad \alpha\sigma > 1.2 \quad \text{Eqn. (3)}$$

$$Z = \dot{\epsilon} \exp\left(\frac{Q}{RT}\right) = A [\sinh(\alpha\sigma)]^n \quad \text{for all stress levels} \quad \text{Eqn. (4)}$$

Where,

$$\alpha = \beta/n',$$

σ is the flow stress (MPa),

A (s^{-1}), β , α (MPa^{-1}), n' and n are material constants at a particular strain.

Table 5 True Stress Values form the Stress Strain graphs at 0.4 strain

Strain rate	True Strain	True Stress (MPa)			
		300 °C	350 °C	400 °C	450 °C
0.001	0.4	39.69	26.94	18.55	13.61
0.01	0.4	47.16	33.09	23.83	18.00
0.1	0.4	61.68	44.86	31.48	24.62
1	0.4	72.10	58.72	43.28	31.61

These are stress values at a particular strain rate and all deformation temperatures which will be further used for the calculation of material parameters and the activation energy from the above proposed method using Zener-Holloman equations.

The derivation of material related constants is presented at the **true strain = 0.4**.

Taking the logarithm of both sides of equation (2) and (3) respectively, it gives:

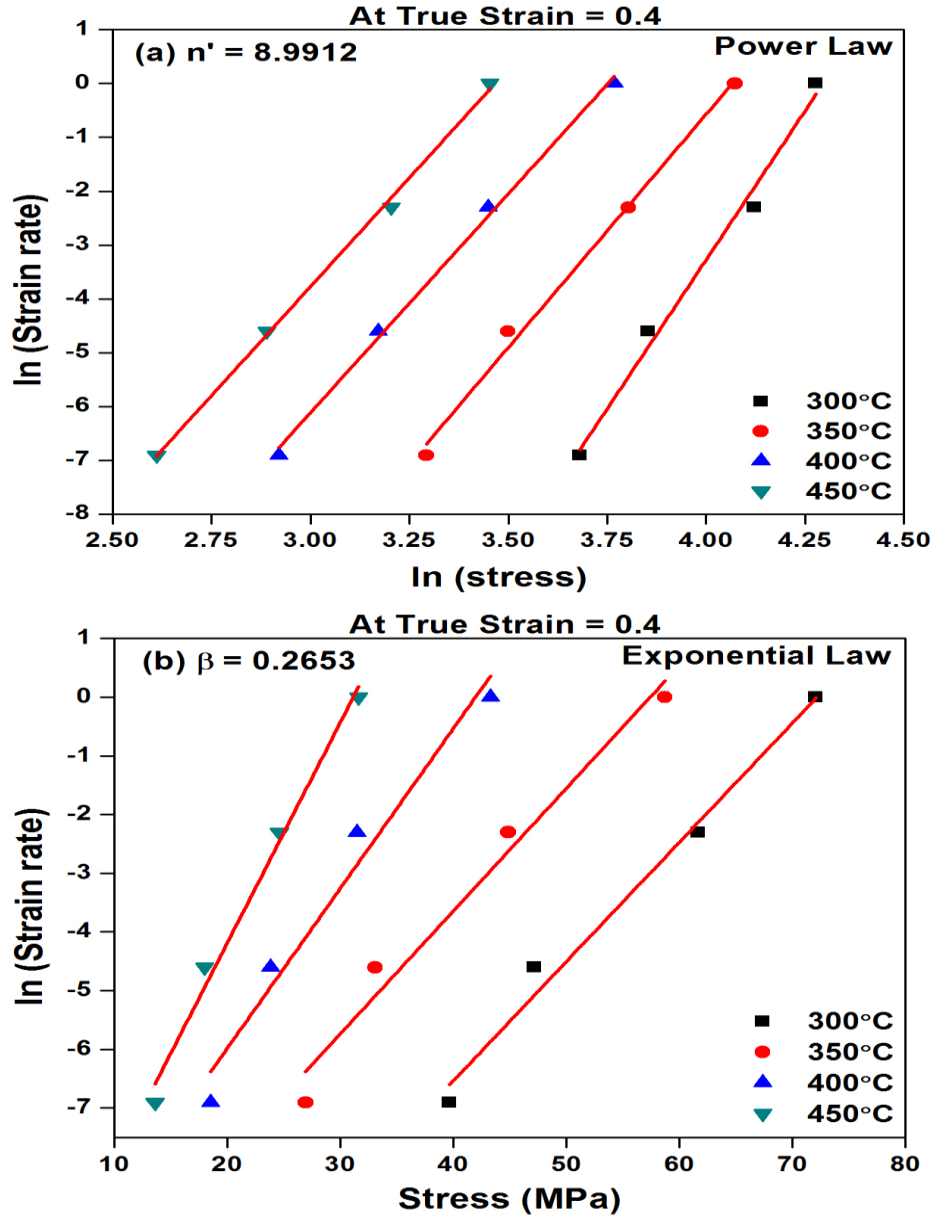
$$\ln \dot{\epsilon} = n' \ln \sigma + \ln A - \frac{Q}{RT} \quad \text{Eqn. (5)}$$

$$\ln \dot{\epsilon} = \beta \sigma + \ln A - \frac{Q}{RT} \quad \text{Eqn. (6)}$$

Fig. 23 (a) shows the dependence of $\ln \dot{\epsilon}$ on $\ln \sigma$ at temperatures of 300 °C, 350 °C, 400 °C and 450 °C respectively. Based on equation (5), the value of n' (at true strain = 0.4) can be derived from the average slope of the lines in $\ln \dot{\epsilon} - \ln \sigma$ plots, which comes out to be 8.9912.

Fig. 23 (b) shows the dependence of $\ln \dot{\epsilon}$ on σ at temperatures of 300 °C, 350 °C, 400 °C and 450 °C respectively. Based on equation (6), the value of β (at true strain = 0.4) can be derived from the average slope of the lines in $\ln \dot{\epsilon} - \sigma$ plots, which comes out to be 0.2653.

Now α can be easily calculated since, $\alpha = \beta/n'$. From the calculation α comes out to be equal to 0.0295.



Now, taking the logarithm of both side of the equation (4), it gives:

$$\ln \dot{\epsilon} = n \ln[\sinh(\alpha\sigma)] + \ln A - \frac{Q}{RT} \quad \text{Eqn. (7)}$$

Using the parameter α derived above, Fig. 23 (c) shows the dependence of $\ln \dot{\epsilon}$ on $\ln[\sinh(\alpha\sigma)]$ at temperatures of 300 °C, 350 °C, 400 °C and 450 °C respectively. Based on equation (7), the value of n (at true strain = 0.4) can be found from the average slope of the lines in $\ln \dot{\epsilon} - \ln[\sinh(\alpha\sigma)]$ plots, which comes out to be 6.476.

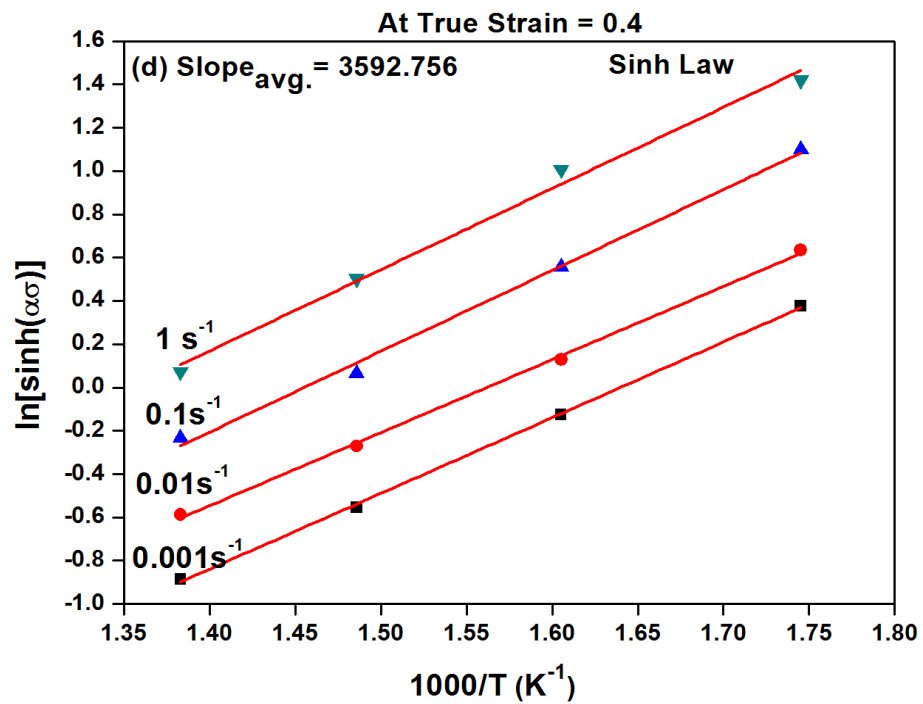
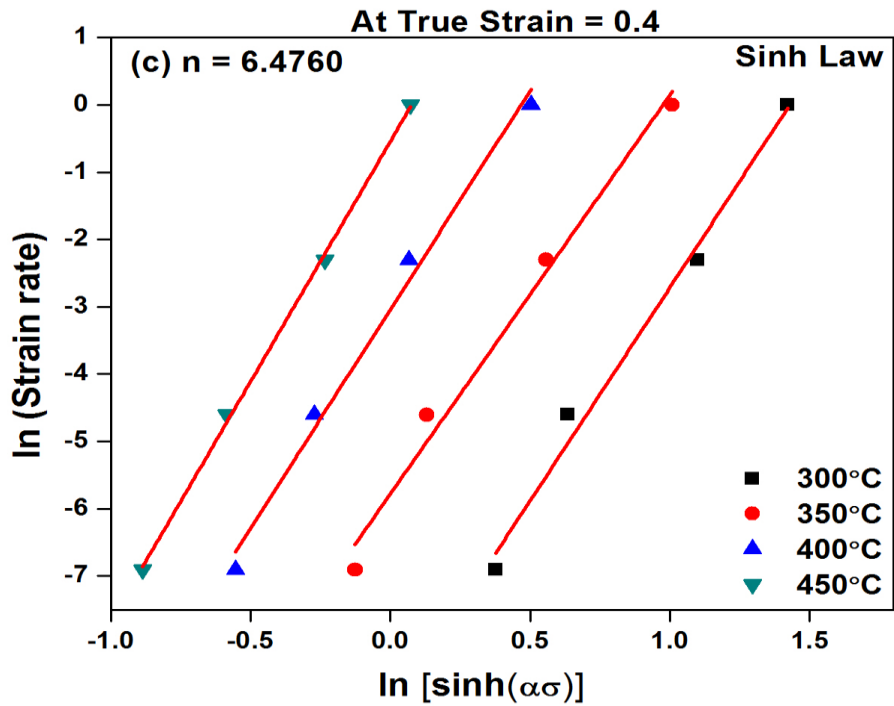


Fig. 23 Evaluating the value of (a) parameter n' by plotting $\ln \dot{\epsilon}$ versus $\ln \sigma$; (b) parameter n' by plotting $\ln \dot{\epsilon}$ versus σ ; (c) parameter n by plotting $\ln \dot{\epsilon}$ versus $\ln[\sinh(\alpha\sigma)]$; (d) the activation energy (Q) using the dependence of $\ln[\sinh(\alpha\sigma)]$ on $(1000/T)$

Now at a given strain rate, the equation (7) is differentiated with respect to $1/T$ which will give us the following equation (8).

$$Q = Rn \frac{d\{\ln[\sinh(\alpha\sigma)]\}}{d(1/T)} \quad \text{Eqn. (8)}$$

Fig. 23 (d) shows the dependence of $\ln[\sinh(\alpha\sigma)]$ on $1000/T$ at strain rates 0.001 s^{-1} , 0.01 s^{-1} , 0.1 s^{-1} , 1 s^{-1} . The average slope of the lines on this graph comes out to be 3.59. Now, on putting the values of all the material constants found above we can get the value of activation energy (Q) from equation (8) which is found to be $193.44 \text{ kJmol}^{-1}$.

Further, using the procedures introduced above, all the material related constants or parameters can be found at different true strains ranging from 0.1 to 0.6 with a specific interval in each case.

However, activation energy value in our work is higher than that for self-diffusion of aluminum 144 kJ/mol [24]. It was also reported that the activation energy for deformation is greater than that for self-diffusion of aluminum in other particulate aluminum composites. The higher activation energy found here might arise to signify the difficulty in plastic deformation caused by the presence of TiB_2 particulates. According to, the higher activation energy for deformation of composites may be due to load transfer to reinforcement from matrix; whereby an interfacial diffusion (along the matrix/ particle interface) can be rate controlling. It is this which is considerably slow and can lead to the higher activation energy for deformation of the present composite.

Further processing maps can be developed to predict the stable and unstable flow regions of materials at elevated temperatures. The details of principles and construction of such maps are summarized in the book by Prasad and Sasidhara. It consists of power dissipation and instability maps, where the former one gives the information of dissipation of power through microstructural changes and the latter gives instabilities of material such as micro cracks and voids. The stable and instable regions of processing map can be identified by the parameters called power dissipation efficiency (η) and instability criteria ($\xi(\dot{\epsilon})$).

5.5.3 SEM Images of composite material after hot deformation at different testing conditions:

Samples after hot compression testing were prepared for the microstructure analysis by using scanning electron microscopy. SEM images of the prepared surfaces of different samples at different testing conditions were taken at two different magnifications. The results shows that the particles are uniformly distributed in the matrix material and also shows some small size reinforcement. The distribution is seen to be a streamline one in different testing conditions. Images for all different testing conditions are shown in figures as follows.

1. At Strain rate 0.001:

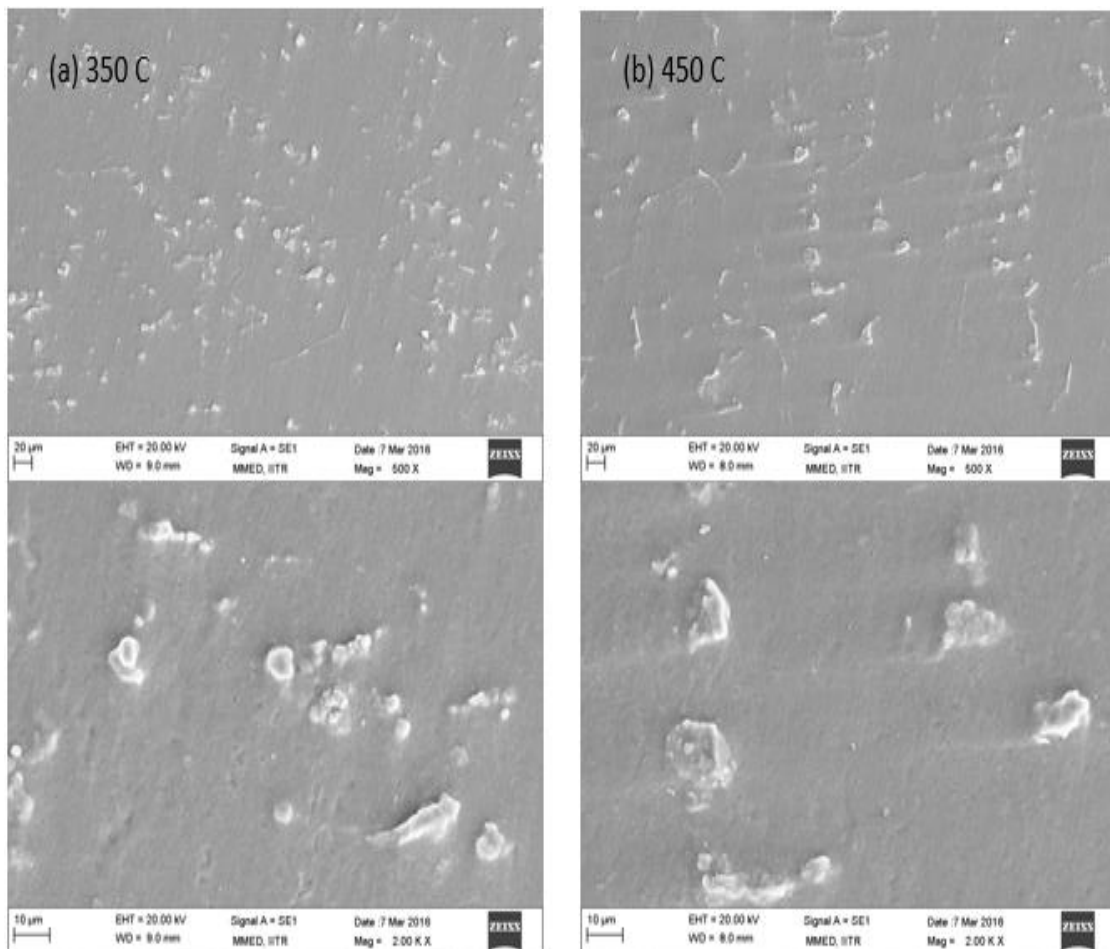
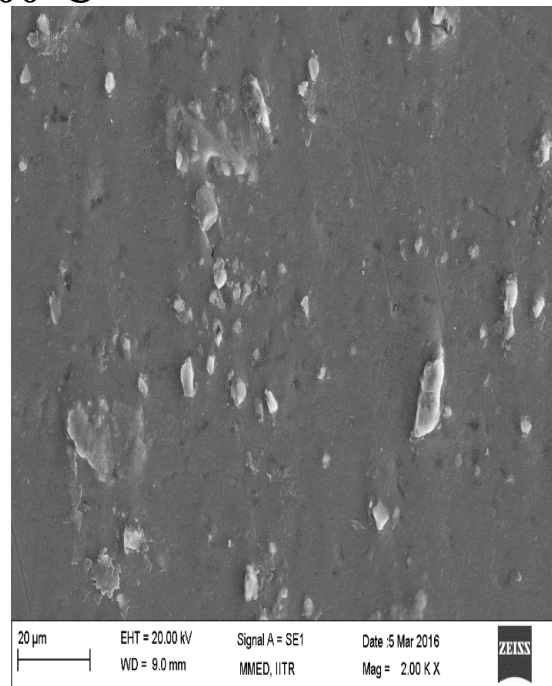
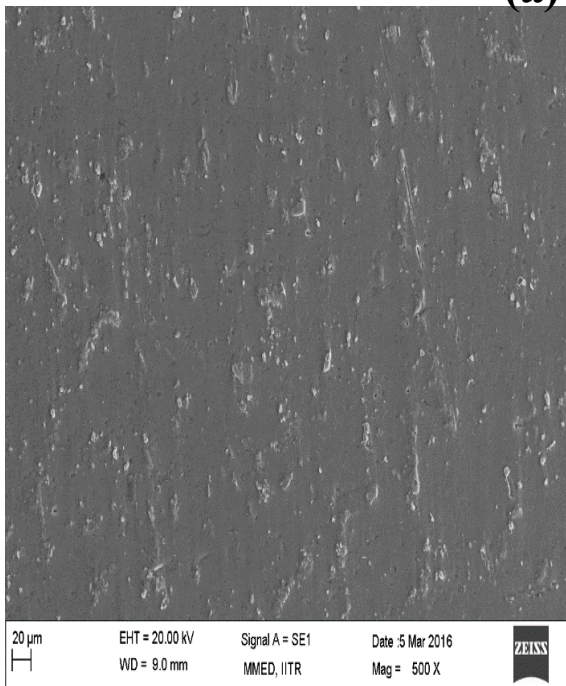


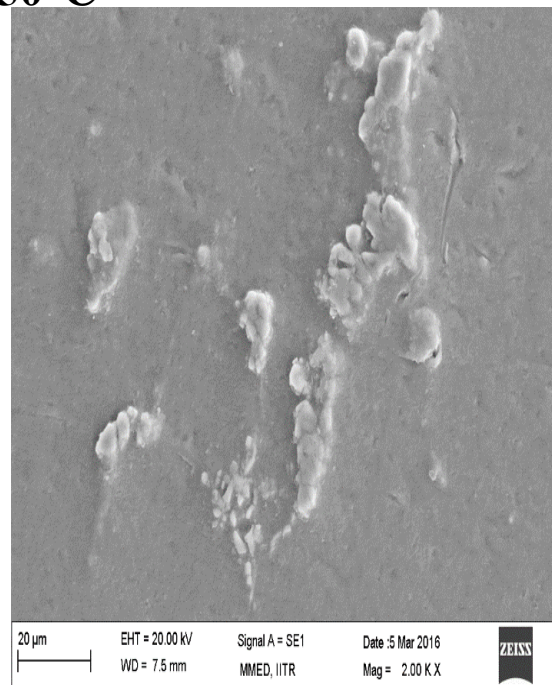
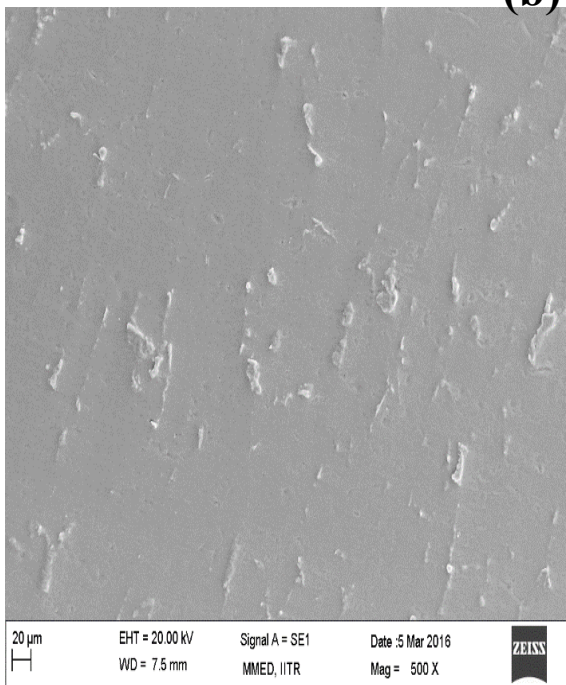
Fig. 24 SEM images of composite after hot deformation at 0.001 strain rate and different temperatures at 500X and 2000X magnification: (a) 350 °C; (b) 450 °C.

2. At Strain rate 0.01:

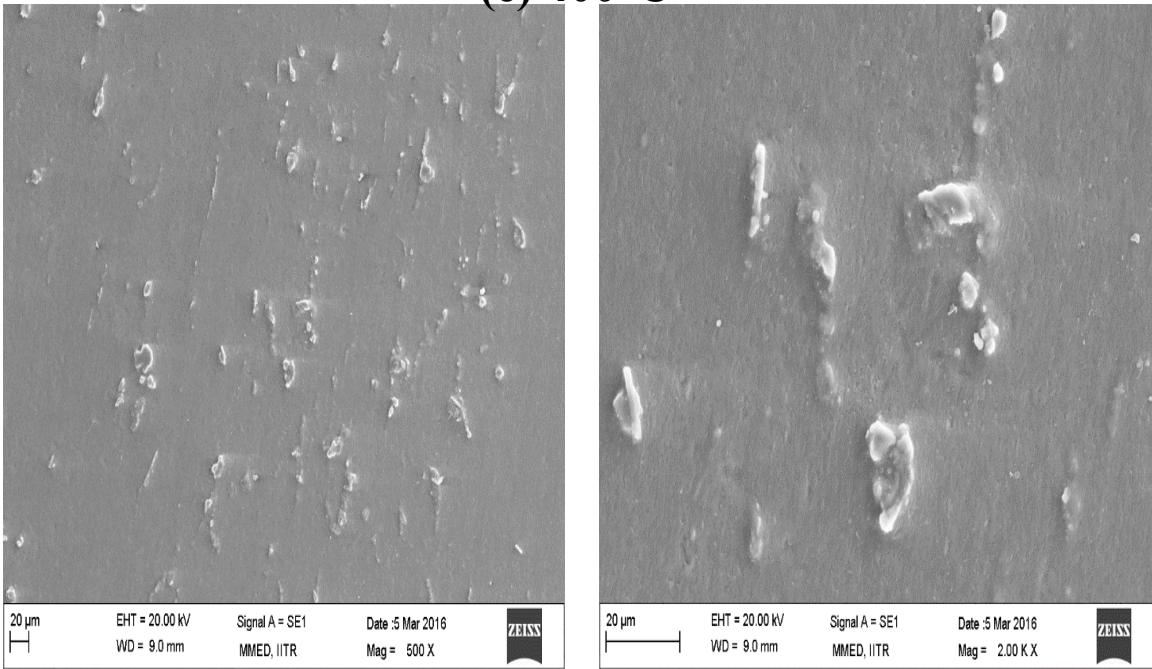
(a) 300°C



(b) 350°C



(c) 400°C



(d) 450°C

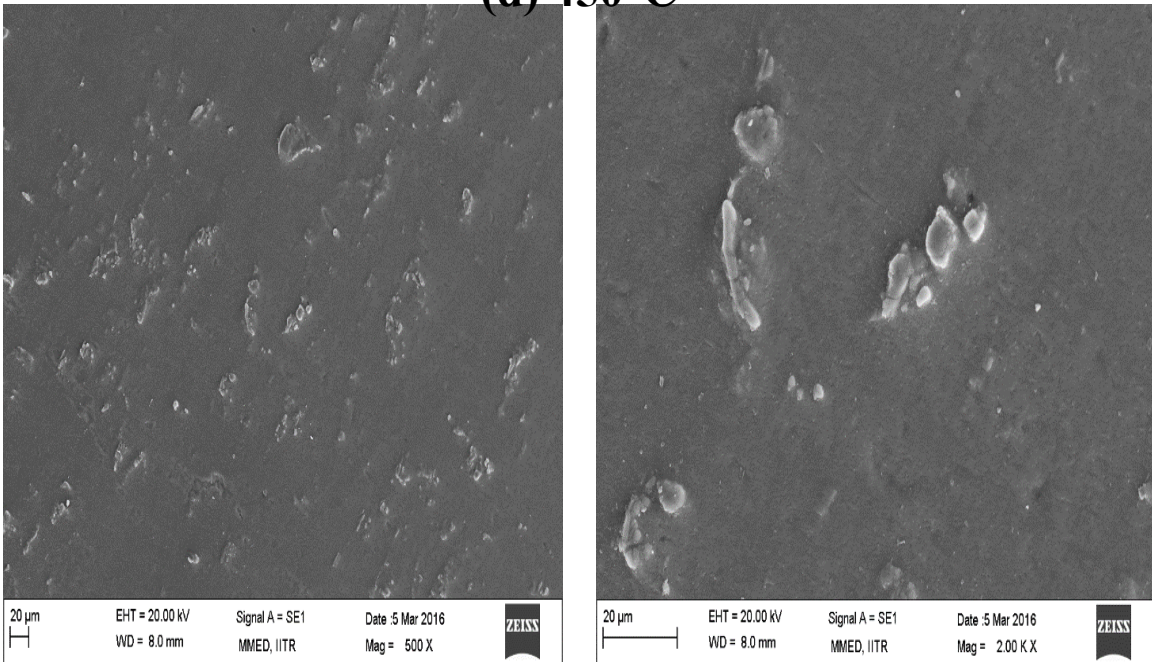
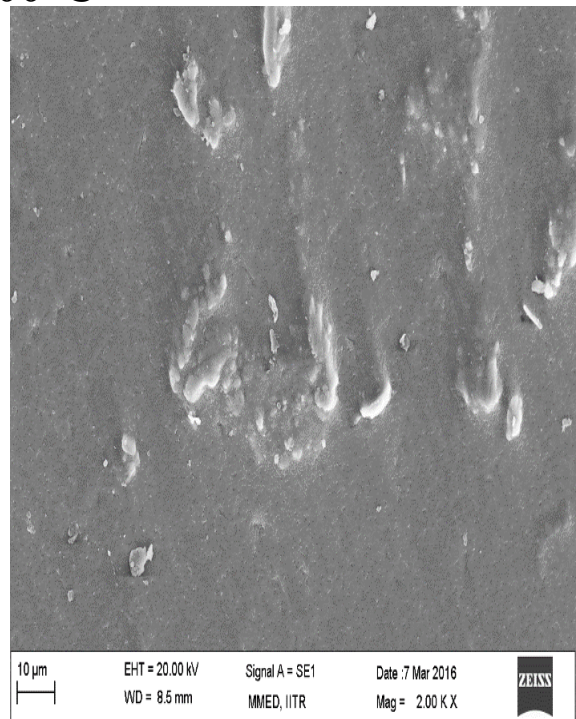
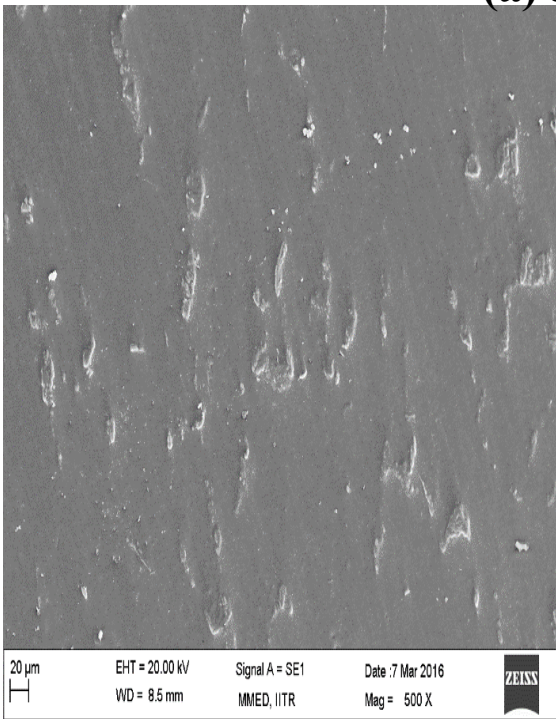


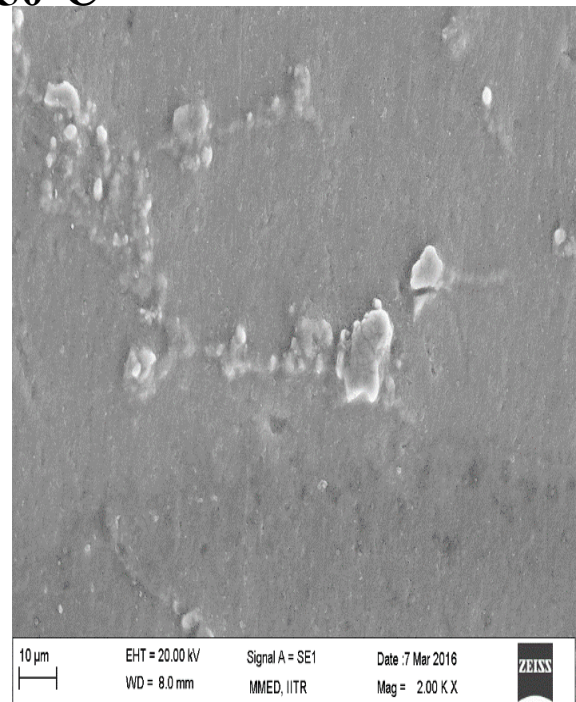
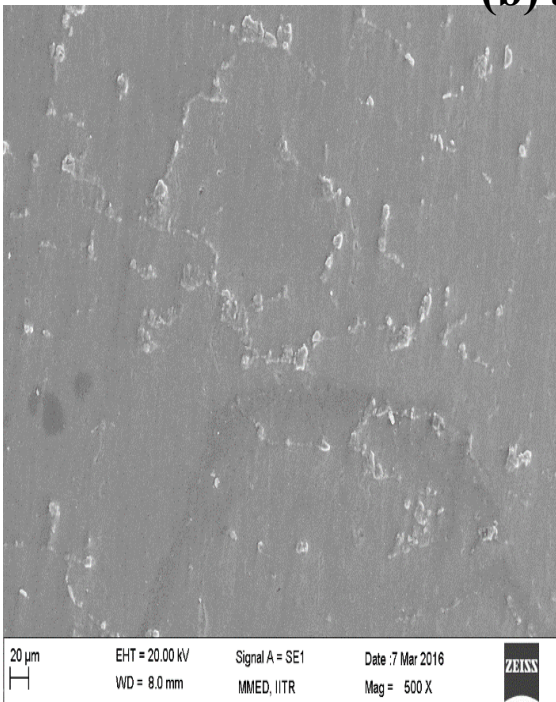
Fig. 25 SEM images of composite after hot deformation at 0.01 strain rate and different temperatures at 500X and 2000X magnification: (a) 300°C; (b) 350°C; (c) 400°C; (d) 450°C.

3. At Strain rate = 0.1:

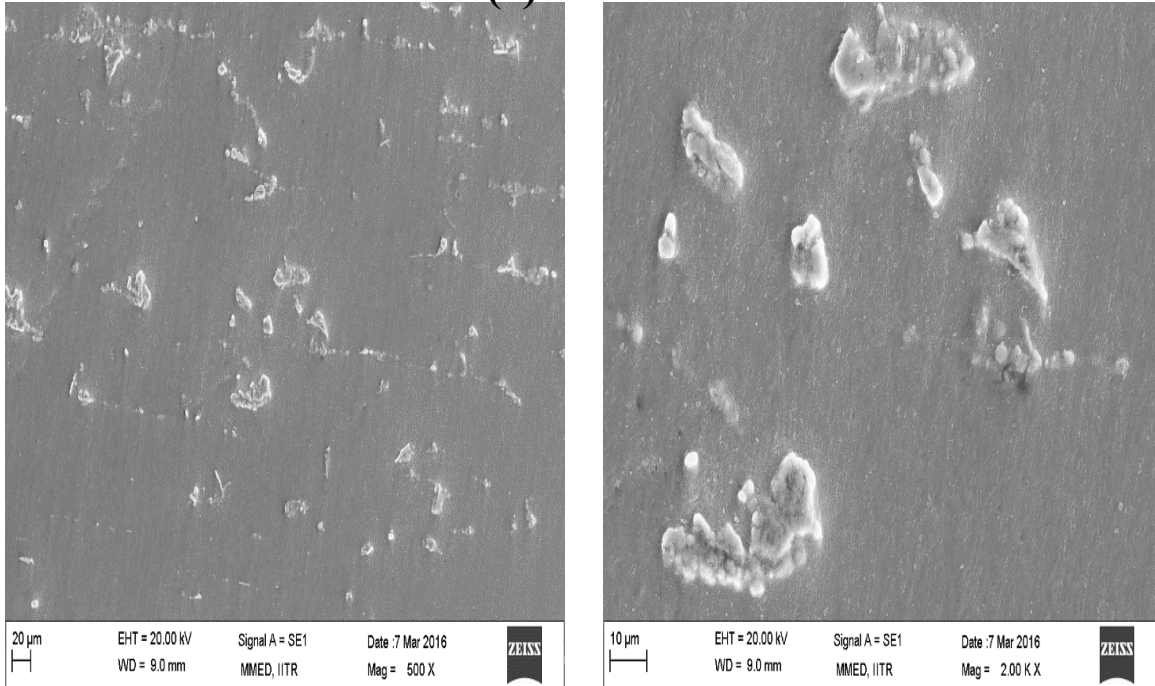
(a) 300°C



(b) 350°C



(c) 400°C



(d) 450°C

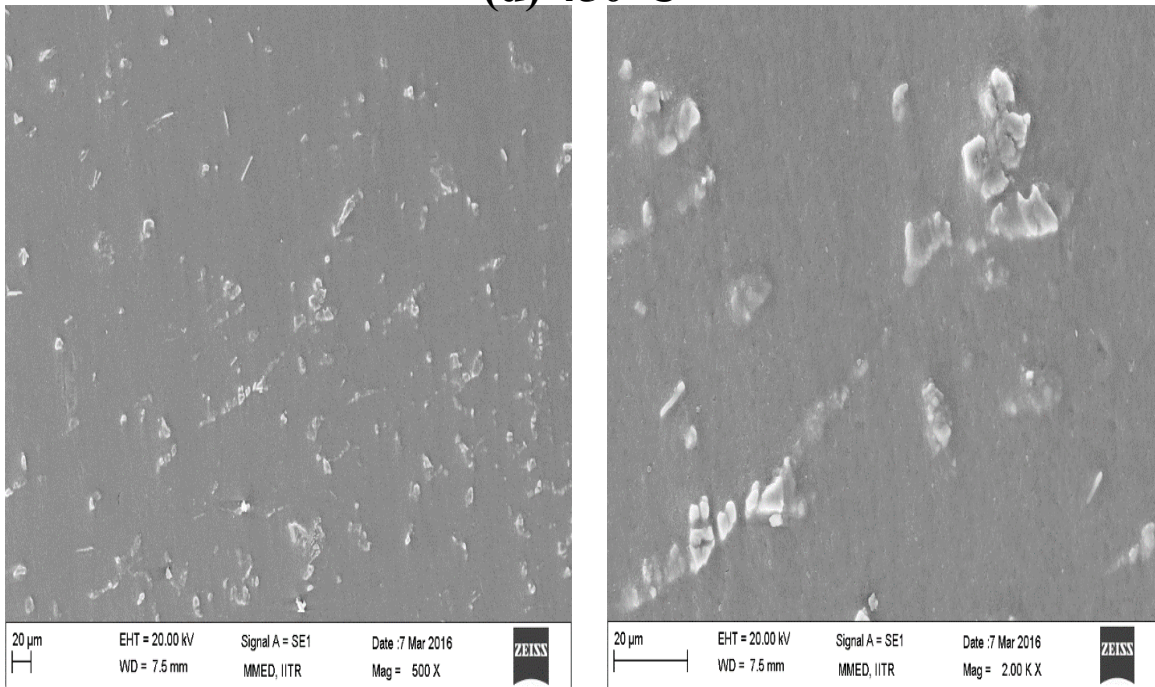
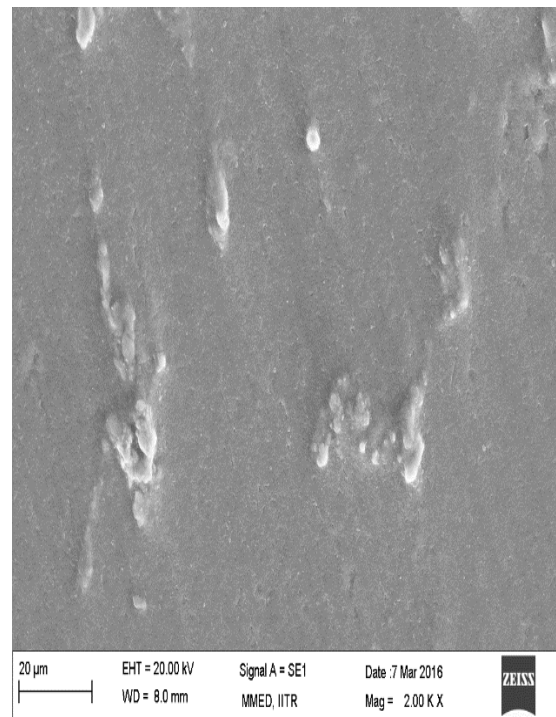
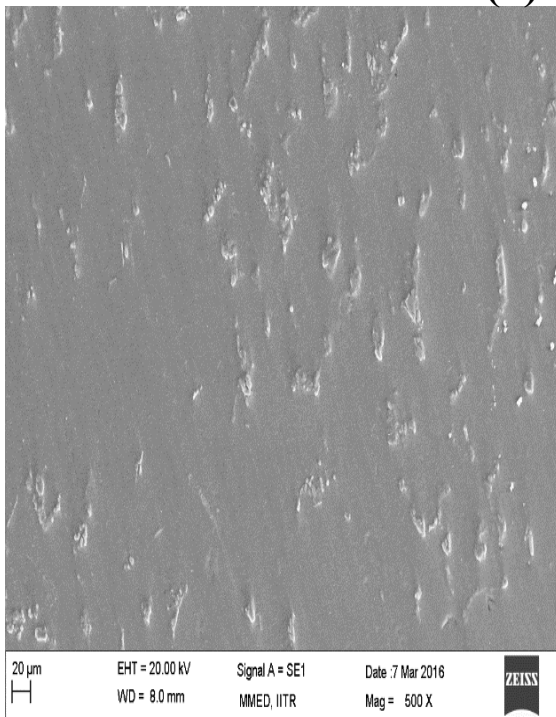


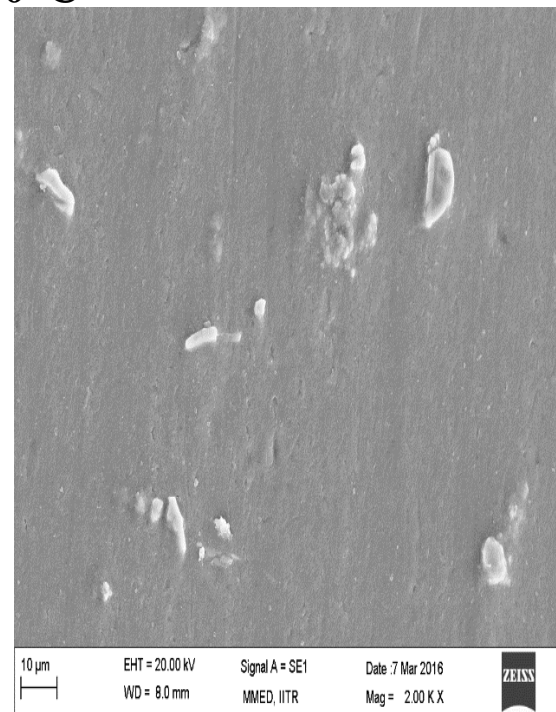
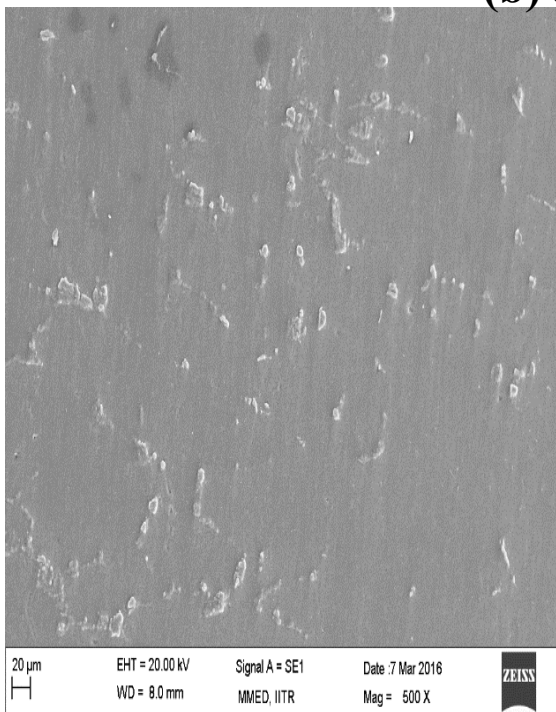
Fig. 26 SEM images of composite after hot deformation at 0.1 strain rate and different temperatures at 500X and 2000X magnification: (a) 300°C; (b) 350°C; (c) 400°C; (d) 450°C.

4. At Strain rate = 1:

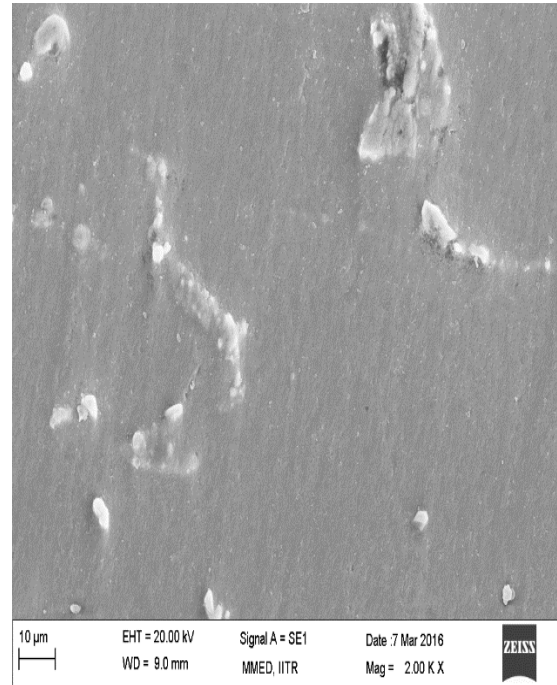
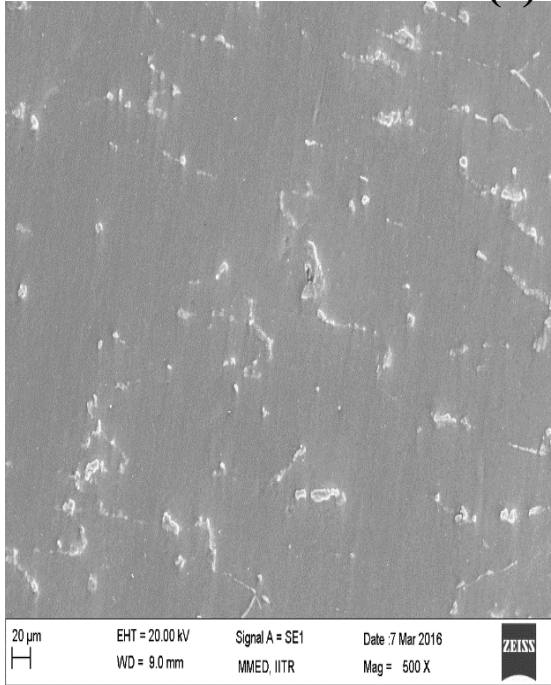
(a) 300°C



(b) 350°C



(c) 400°C



(d) 450°C

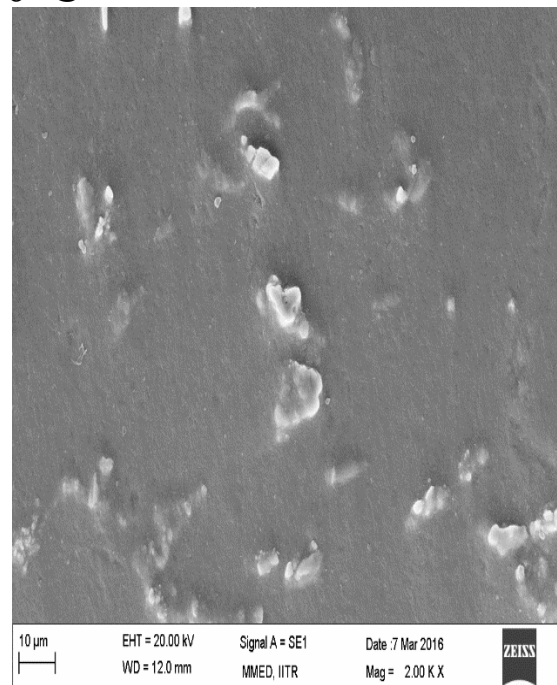
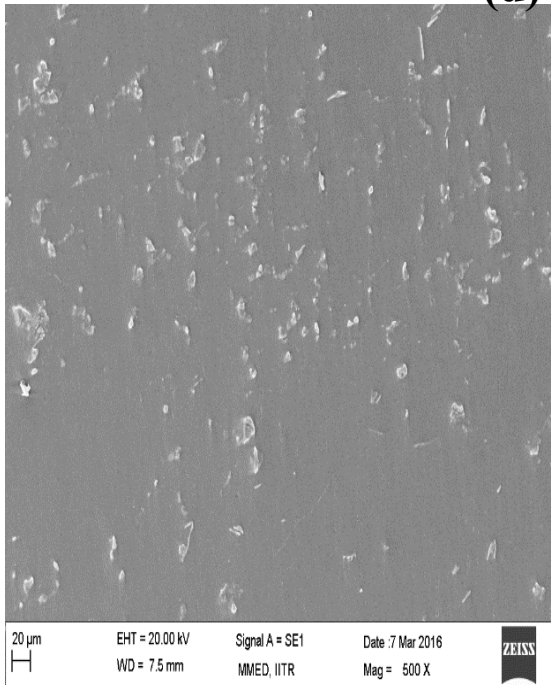


Fig. 27 SEM images of composite after hot deformation at 1 strain rate and different temperatures at 500X and 2000X magnification: (a) 300°C; (b) 350°C; (c) 400°C; (d) 450°C.

- Al6061-5 wt. % TiB₂ composite is successfully produced by in-situ process using ultrasonic assisted stir casting technique.
- Tensile strength and hardness of the Al6061-5 wt. % TiB₂ composite is recorded higher than the base alloy.
- Hot deformation tests was done in the strain rate range 0.001 to 1 s⁻¹ and temperature ranging from 300°C to 450°C.
- True stress – True strain plots are drawn which shows that flow stress increases with the increase in strain rate and decrease in the deformation temperature.
- A constitutive model describing the relationship of the flow stress, true strain, strain rate and temperature is proposed. The coefficients (E.g., β , α (MPa⁻¹), n' , n , Q) in the constitutive equation of model are functions of true strains.
- Hot deformation activation energy is found to be 193.44 kJmol⁻¹.
- SEM images before and after the hot deformation tests shows the presence and distribution of TiB₂ particles.
- Microstructural evolution or changes are well explained by the SEM analysis of hot deformed composites.

CHAPTER 7

FUTURE SCOPE

- From the data we obtained, processing maps can be drawn to get the regions of safe forming for combinations of process parameters such as deformation temperature and strain rate. Also, the instable regions can be found.
- Metal forming operations like rolling, forging, extrusion can be done to further study and improve the workability.
- Reinforcement weight % can be varied, studied for workability and then analyzed by comparing with the results of this work.
- Workability study and determination of activation energy can be done for another matrix material composite and compared with these results.

REFERENCES

1. Daniel B. Miracle and Steven L. Donaldson: Introduction to Composites, ASM Hand Book of Composite Materials, 2010, vol. 21, pp. 434-440.
2. S.L.Kakani, Amit Kakani: Material science, New Delhi, New age international publishers, 2004, pp. 593-613.
3. J. W. Martin: Materials for Engineering, Wood Head Publishing Limited, England, 2008, pp. 189.
4. H. Kala, K.K.S Mer, S. Kumar: A Review on Mechanical and Tribological Behaviors of Stir Cast Aluminum Matrix Composites, Procedia Materials Science, 2014, vol. 6, pp. 1951 – 1960.
5. Johny James.S, Venkatesan.K, Kuppan.P, Ramanujam.R: Comparative Study of Composites Reinforced With SiC and TiB₂, Procedia Engineering, 2014, vol. 97, pp. 1012 – 1017.
6. R. S. Rana, Rajesh Purohit, S.Das: Review of recent Studies in Al matrix composites, ISSN, 2012, vol. 3, pp. 2229-2245.
7. S. Suresh, N.S.V. Moorthi: AMMCs, Challenges and Opportunities, Procedia Engineering, 2012, vol. 38, pp. 98-97.
8. Z. Liua,, Qingyou Han, Jianguo Li, Weidong Huang: Effect of ultrasonic vibration on microstructural evolution of the reinforcements and degassing of in situ TiB₂p/Al–12Si–4Cu composites, Journal of Materials Processing Technology, 2012, pp. 365– 371.
9. T.V. Christy, N. Murugan, S. Kumar: A Comparative Study on the Microstructures and Mechanical Properties of Al 6061 Alloy and the MMC Al 6061/TiB₂/12P, Minerals & Materials Characterization & Engineering, 2010, vol. 9, pp. 57-65.
10. Srivatsan T.S., Meslet Al-Hajai, B. Hotton and P. C. Larn: Effect of Particulate Silicon Carbide on Cyclic Plastic Strain Response and Fracture Behaviour of 6061 Aluminium alloy MMC, Applied Composite Materials, 2002, pp. 131-153.
11. Feng C.F., Froyen, L: Microstructure of in-situ Al/TiB₂ MMCs Prepared by a Casting Route, Journal of Material Sciences, 2000, vol. 35, pp. 837-850.

12. C.S. Ramesh, S. Pramod, R. Keshavamurthy: A study on microstructure and mechanical properties of Al 6061–TiB₂ in-situ composites, *Materials Science and Engineering A*, 2011, vol. 528, pp. 4125-4132.
13. Y. M. Yousef, R.J. Dashwood, P.D. Lee: Effect of Clustering on Particle Pushing and Solidification Behaviour in TiB₂ Reinforced Al PMMCs, *Composites*, 2005, vol.36 (A), pp. 747-763.
14. Yuyoung chen, Chung, D. D.L: In-Situ Al-TiB₂ Composite Obtained by Stir Casting, *Journal of Material science*, 1996, vol. 31, pp. 311-315.
15. Mohamed A. Taha, Nahed A. El-Mahallawy, Ahmed M. El-Sabbagh: Some experimental data on workability of aluminium particulate reinforced metal matrix composites, *Journal of materials processing technology*, 2008, vol. 202, pp. 380–385.
16. J. Jiang, B. Dodd: Workability of aluminium-based metal matrix composites in cold compression, *Composites*, 1994, vol. 26, pp. 62-66.
17. M. Rajamuthamil sevlan, S. Ramamathan: Effect of SiC volume fraction on the hot workability of 7075 Al metal-matrix composites, *International Journal Manufacturing and Technology*, 2013, pp. 1711-1720.
18. Prasad YVRK, Rao KP: Processing maps and rate controlling mechanisms of hot deformation of electrolytic tough pitch copper in the temperature range 300–950 °C, *Material Science Engineering*, 2005, vol. A 39, pp. 1141–150.
19. Huizhong Li, Haijun Wang, Min Zeng, Xiaopeng Liang, Hongting Liu: Forming behavior and workability of 6061/B₄CP composite during hot deformation, *Composites Science and Technology*, 2011, vol. 71, pp. 925–930.
20. Zhang, F. Li, and Q. Wan: Constitutive Equation and Processing Map for Hot Deformation of SiC Particles Reinforced Metal Matrix Composites, *J. Mater. Eng. Perform*, 2010, pp. 1290-1297.
21. S. Gangolu, A.G. Rao, N. Prabhu, V.P. Deshmukh, and B.P. Kashyap: Hot Workability and Flow Characteristics of Aluminum-5 wt. % B₄C Composite, *JMEPEG*, 2014, pp. 1366–1373.

22. Do-Hyun Park, Byung-Chul Ko, Yeon-Chul Yoo: Evaluation of Hot Workability of particle reinforced composites by using deformation efficiency, *Journal of Material Science*, 2002, vol. 37, pp. 1593-1597.
23. Aruna Patel, S.Das, B.K. Prasad: Compressive deformation behavior of Al2014-10 wt% SiC composite, *Materials Science and engineering*, 2011, vol. A 530, pp. 225-232.
24. S. Gangolu, A.G. Rao, N. Prabhu, V.P. Deshmukh, and B.P. Kashyap: Hot Workability and Flow Characteristics of Aluminum-5 wt.% B4C Composite, *Journal of Materials engineering and performance*, 2014, vol. 23, pp. 1366-1373.